LEVEL 2:
BE INTERESTING.

THESE ARE YOUR FRIENDS.

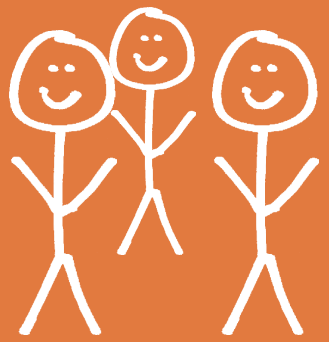

(OR COLLEAGUES.)

LEVEL 2:
BE INTERESTING.

THESE ARE YOUR FRIENDS.

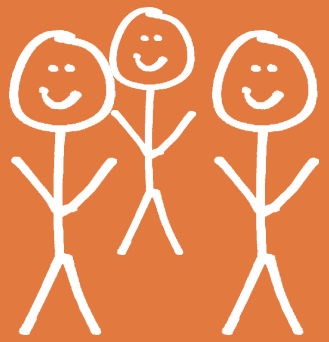

(OR COLLEAGUES.)

They want to support you but don't want to be bored.

LEVEL 2:
BE INTERESTING.

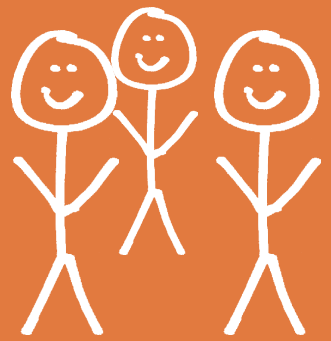

LEVEL 2:
BE INTERESTING.

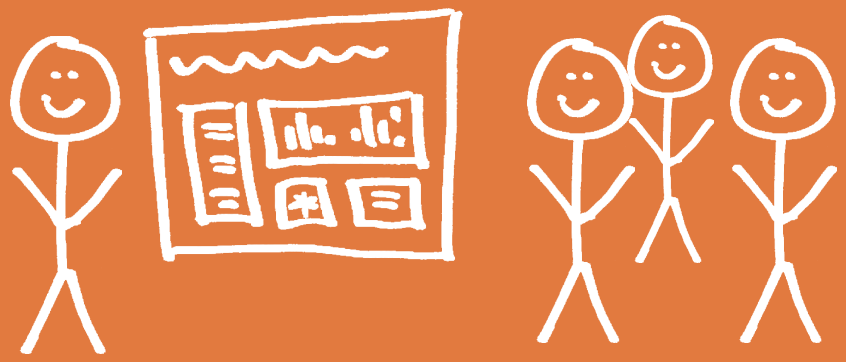

1. WOW WITH A TITLE.
2. BIG IMAGES, SIMPLE GRAPHS.
3. PULL QUOTES, KICKERS, ETC.

POINTS OF ENTRY


POINTS OF ENTRY

POINTS OF ENTRY

- TITLE
- HEADINGS
- IMAGES
- GRAPHS
- CAPTIONS
- KICKERS
- PULL QUOTES

LEVEL 2:
BE INTERESTING.

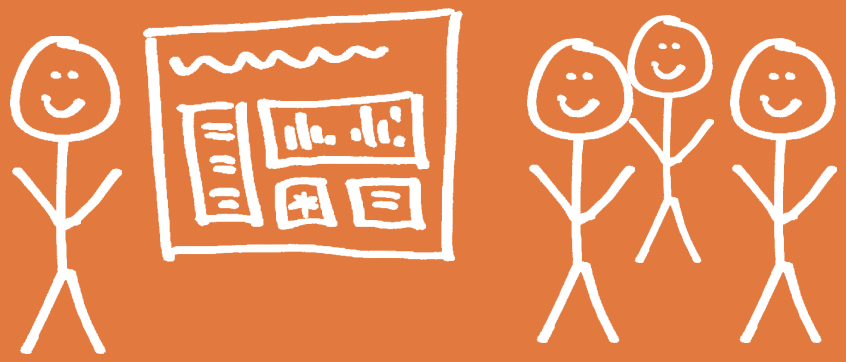

1. WOW WITH A TITLE.

These Little Guys Eat Asphaltenes During Starvation

Hossein Jahromi
Department of Biological Engineering, Utah State University

Background

Utilization of plastic containers caused severe environmental concerns.

Application of microorganisms for environmental remediation was proposed 100 years ago.

Beckam, 1926, brought microorganisms into petroleum field on EOR porpuses.

Research Abstract

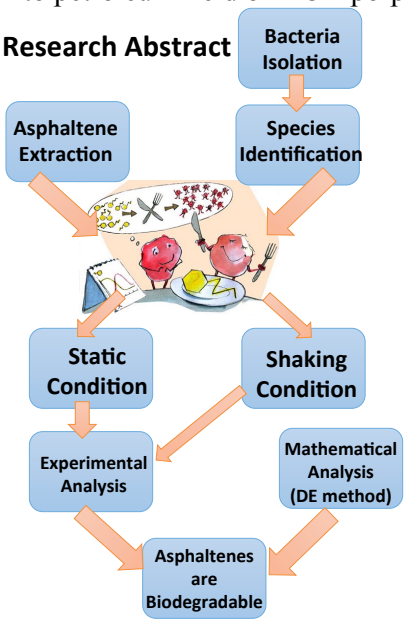

Objectives

1. Isolation of microorganisms that are capable of degrading asphaltenes
2. Assessment of biodegradability of asphaltenes under shaking and static conditions
3. To study the kinetics of asphaltene biodegradation

Identified Species

Gram test	Growth condition	Accession number	Source	Species type	
Gram negative	Optional Anaerobic	EU310372	Shiraz Refinery Oil-contaminated Soil	Pseudomonas Fluorescence	Cons.1
Gram negative	Optional Anaerobic	HM748462	Shiraz Refinery Oil-contaminated Soil	Enterobacter Cloacae	
Gram negative	Optional Anaerobic	GQ426323	Shiraz Refinery Oil Sludge	Enterobacter Cloacae	Cons.2
Gram negative	Aerobic	DQ071568	Shiraz Refinery Oil Sludge	Bacillus licheniformis	
Gram positive	Aerobic	JN575344	Assaluye Refinery Contaminated Soil	Bacillus firmus	Cons.3
Gram negative	Optional Anaerobic	AE004091	Assaluye Rerinery Oil Sludge	Pseudomonas aeruginosa	Cons.4

Biodegradation Results

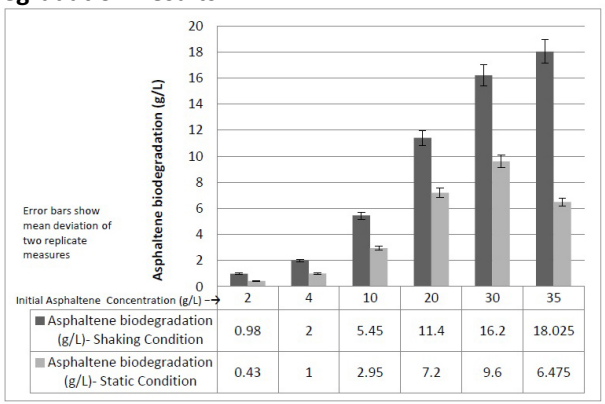

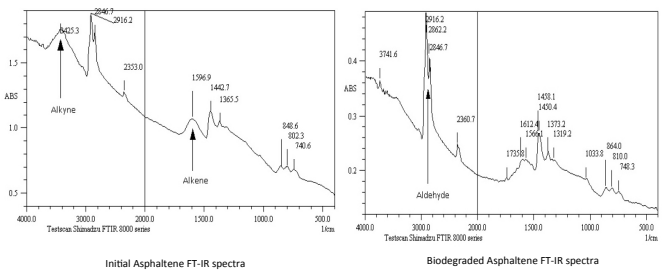

Initial Asphaltene FT-IR spectra

Biodegraded Asphaltene FT-IR spectra

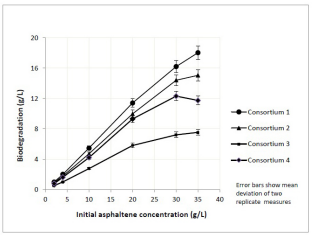

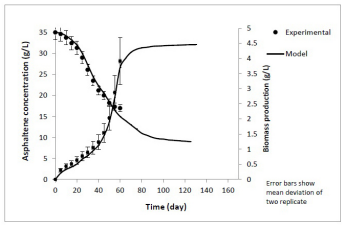

Tessier Model

$$\mu = \mu_{max}(1 - e^{-\frac{s}{ks}})$$

$$\frac{dx}{dt} = \mu \times x$$

$$\frac{ds}{dt} = -\frac{\mu \times x}{Y_{xs}}$$

$Y_{X/S}$	K_s	$_{max}\mu$	% Biodegradation	Consortium	Fermentation mode
0.202	24.17	0.42	57	Cons.1	Aerobic shaking condition
0.20	27.61	0.36	49.8	Cons.2	
0.189	42.6	0.29	29	Cons.3	
0.20	26.75	0.31	46.5	Cons.4	
0.226	33.43	0.39	36	Cons.1	Aerobic mixed condition
0.284	34.19	0.38	32.2	Cons.2	
0.281	46.66	0.29	17	Cons.3	
0.215	32.66	0.32	33.5	Cons.4	

Conclusions

- Biodegradation was proportional to initial asphaltene concentration
- Asphaltene biodegradation is of higher rate under shaking condition in comparison with static condition
- Asphaltene structure plays a central role in biodegradability according to FT-IR spectra
- Asphaltene biodegradation data in all experiments fitted to Tessier kinetic model

Future Works

- Investigation of asphaltene biodegradation in different environmental media such as sea water and soil
- Assessment of asphaltene biodegradation mechanism and identification of reaction pathways

hossein.jahromi@aggiemail .usu.edu

THESE LITTLE GUYS EAT ASPHALTENES DURING STARVATION

Investigating mesospheric gravity wave dynamics over McMurdo Station, Antarctica (77° S)

Jonathan R. Pugmire, Mike J. Taylor, Yucheng Zhao, P.-Dominique Pautet
Center for Atmospheric and Space Sciences, Utah State University

Introduction

The Antarctic Gravity Wave Instrument Network (ANGWIN) is an NSF sponsored international program designed to develop and utilize a network of gravity wave observatories using existing and new instrumentation operated at several established research stations around the continent. Utah State University's Atmospheric Imaging Lab operates all-sky infrared imagers at several research stations. Here we present novel measurements of short-period and larger-scale mesospheric gravity waves imaged during 2012 from McMurdo Station (77.8°S, 166.7°E) on Ross Island. This IR camera has operated at Arrival Heights alongside the University of Colorado Fe Lidar during the past three winter seasons (March-September 2012-2014). Two initial primary goals are:

- Quantify the properties of small- and medium-scale mesospheric gravity wave climatology over this region of Antarctica.
- Combine results with similar measurements from other ANGWIN stations to investigate continental-wide gravity wave dynamics (see SA31B-4100).

IR Imaging

All-sky observations of the OH emission layer (~87 km) were made using an infrared (0.9-1.7 μm) cooled InGaAs camera. The OH airglow emissions are much stronger in the infrared region (>1 μm), as shown in blue in the figure to the right, and we use new InGaAs cameras to obtain high-quality short-exposure images of gravity waves under auroral and full moon observing conditions.

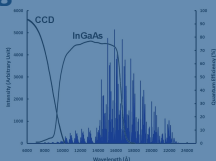

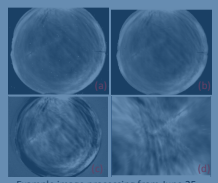

Example image processing from June 25, 2012, 09:57 UT.

Raw all-sky (180°) OH image data were recorded every 10 s with a 3 s exposure enabling detailed measurements of individual gravity wave events.
(a) Raw image oriented using the IR star field.
(b) Stars removed
(c) Flat fielded: Average nightly image subtracted.
(d) Unwarped to 350 x 280 km geographic grid at 87 km altitude.

Optical site at Arrival Heights, McMurdo Station

Gravity waves were analyzed using well-developed Fourier analysis techniques to determine direction of propagation (θ), horizontal wavelength (λ), observed horizontal phase speed (*v*) and wave period (T) [e.g. Taylor, et al, 1997].

During the 2012 observing period (March-September, nighttime hours) at McMurdo over 400 short-period (<1 hr) gravity wave events were observed.

Large-Scale Tidal Analysis

A **low-pass filter (>1 hr periods)** of the large 73 hour keogram revealing strong tidal features with characteristic periods as identified in the FFT analysis.

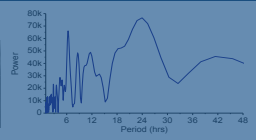

FFT power spectrum analysis identifying mesospheric tidal signatures. Note the strong diurnal tide at 24 hours and several harmonics at 6, 8, and 12 hrs.

Two Awesome Weeks in August

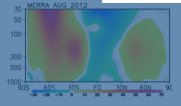

Zonal Mean Wind: Eastward winds throughout the stratosphere (77°S) create a critical layer for eastward wave phase speeds less than ~30 m/s [MERRA].

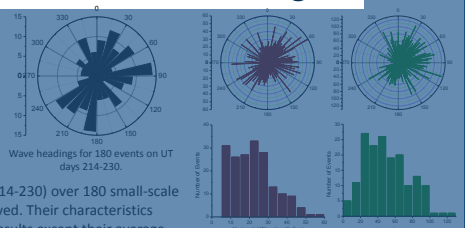

Wave headings for 180 events on UT days 214-230.

On August 2-18, 2012 (UT day 214-230) over 180 small-scale gravity wave events were observed. Their characteristics were similar to the full season results except their average phase speeds (50 m/s) were significantly higher. These wave events dominated the end of season results. The phase speed distribution is consistent with critical level wind-filtering [Nielson, et al, 2012] with much higher eastward phase speeds.

Three Continuous Days in June

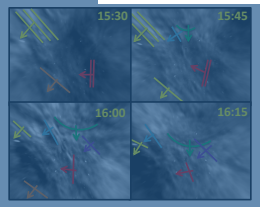

The four unwarped images above show example 350 x 280 km airglow images taken on day 176 every 15 minutes revealing both the high level of wave activity and quality of the images. Several wave features are highlighted as they propagate through the images. The blue and green lines can also be seen in keogram data below, wave event #1.

In mid-winter there is continuous darkness at McMurdo. From June 23-26, 2012 (day 175-178) over 40 small-scale gravity wave events were analyzed during 73 continuous hours of observations. Their properties are shown in the figures below.

Observed Wavelength Note the prevailing NE and SW wave motions, similar to the winter summary plot.

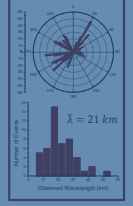

Observed Phase Speed Note the large spread and preferential direction of waves with higher phase speeds.

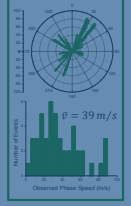

Observed Period The black line is a power spectrum of the keogram using a high-pass (<60 min) filter and shows good agreement.

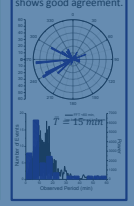

Keograms

Both large- and small-scale gravity wave features can be studied by creating keograms. A keogram is made by stacking vertical (and horizontal) slices through the center of each image together to form a time series revealing wave activity as a function of time. The large keograms along the bottom of the poster shows 73 continuous hours of wave data starting (day 175, 01:33 UT to day 178, 03:09 UT). These data illustrate the high quality of our gravity wave measurements from Antarctica.

Small-Scale Gravity Waves

A **high-pass filter** was applied to the keogram to measure small-scale gravity waves with periods of 5-60 min (as highlighted in yellow boxes). Two selected wave events are shown together with their FFT power spectrum. These are compared with the event properties analyzed from the individual airglow images.

Wave Event #1: Day 176, 15:30-19:00
λ = 22 ± 3 km θ = 217° ± 5°
v = 44 ± 5 m/s T = 8 ± 3 min

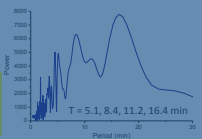

Wave Event #2: Day 177, 16:50-20:00
λ = 24 ± 3 km θ = 318° ± 5°
v = 42 ± 5 m/s T = 10 ± 3 min

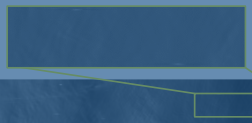

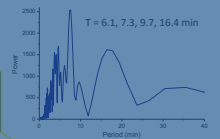

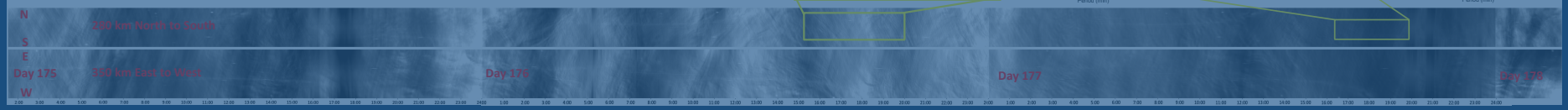

Summary: 2012 Wave Parameters

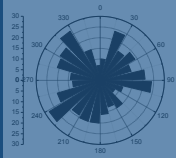

Distribution of Wave Headings: Winter season wave motions were prominent in several directions.

The data show evolution from NW propagation (107 events) in the fall which expands to NE and SW wave motions during mid-winter (110 events). The late winter was dominated by many waves (202 events) again exhibiting strong NE and SW motions but more isotropic than earlier. The strong asymmetries are suggestive of localized sources.

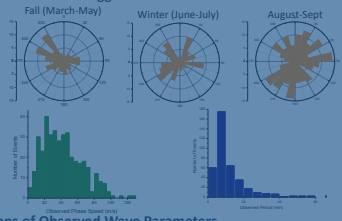

Distributions of Observed Wave Parameters

A total of 419 events were analyzed. Their average values were λ= 22 km, *v* = 42 m/s, T = 12 min. These mean values and their ranges are typical for short-period gravity waves observed at several sites around Antarctica as part of ANGWIN.

Summary

We have analyzed one year of data to date from McMurdo Station, Antarctica. The results are as follows:

- A large number (400+) of short-period gravity waves observed over McMurdo, Antarctica enabling the wintertime mesosphere wave climatology to be investigated for the first time.
- McMurdo waves exhibits a large spread of phase speeds with a tendency for high phase speeds up to ~120 m/s.
- New keogram analysis enables the investigation of larger period gravity waves and tidal perturbations in the mesosphere revealing 6, 8, 12, and 24 hr tides and harmonics.
- The sources of the wave events observed from McMurdo are probably associated with strong localized weather systems associated with the polar vortex.
- Small-scale wave event analysis results are comparable using FFT and keograms.

Sketch illustrating direction of propagation from McMurdo

Future Work

- Ongoing measurements from the South Pole station in combination with other ANGWIN sites will be used to investigate pan-Antarctic anisotropy and wave parameters.
- New analysis of McMurdo data from 2013 and 2014 data will further clarify the asymmetries in the wave propagation at this site for understanding the climatology of gravity waves observed at McMurdo.
- Comparison with onsite Fe Boltzmann Lidar measurements and MF radar wind measurements.

References

MERRA Atlas, GEOS-5, August 2012, NASA Goddard Space Flight Center, Retrieved December 11, 2014.

Nielsen, K., Taylor, M. J., Hibbins, R. E., Jarvis, M. J., & Russell, J. M. (2012). On the nature of short-period mesospheric gravity wave propagation over Halley, Antarctica. *Journal of Geophysical Research: Atmospheres (1984–2012)*,*117*(D5).

Taylor, M.J., W.R. Pendleton, Jr, S. Clark, H. Takahashi, D. Gobbi, and R.A. Goldberg (1997). Image measurements of short-period gravity waves at equatorial latitudes, *J. Geophys. Res., 102*, 26,283-26,299.

Acknowledgements This research was supported by NSF grant ANT-1045356.

Two Awesome Weeks in August

Three Continuous Days in June

LEVEL 2:
BE INTERESTING.

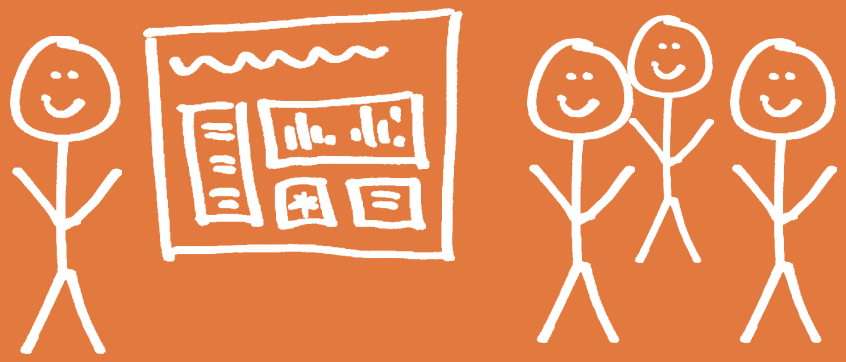

1. WOW WITH A TITLE.

2. BIG IMAGES, SIMPLE GRAPHS.

TransJ: Framework-Independent abstractions for Weaving Crosscutting Concerns into Distributed Transactions in AspectJ

Anas M.R AlSobeh, Stephen W Clyde

Utah State University

Abstract

Implementing crosscutting concerns for transactions is difficult, even using Aspect-Oriented Programming Languages (AOPL) such as AspectJ. Many of these challenges are because the context of transaction-related crosscutting concern is often a context consisting of loosely-coupled abstractions like dynamically generated identifiers, timestamps, and tentative value sets for distributed resources. Current AOPL do not provide joinpoints and pointcuts for weaving of advice into high-level abstractions, like transactions. Other challenges stem from essential complexity in the nature of the data, operations on the data, or the volume of data, and accidental complexity comes from the way that the problem is being solved even using common transaction frameworks. This paper describes an extension to AspectJ, called *TransJ*, with which developers can implement transaction-related concerns in cohesive and loosely coupled aspects. It also presents a preliminary experiment that we hope will provide evidence of improvement in reusability without sacrificing performance of applications requiring transactions.

Achieving Good Quality Software

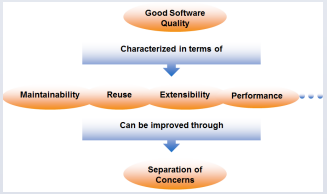

Objective

An extension for AspectJ to weave transaction-related crosscutting concern into a DTPS in a modular and reusable way, while preserving the performance, core functionality, and obliviousness to those concerns.

Sample of Crosscutting Concerns

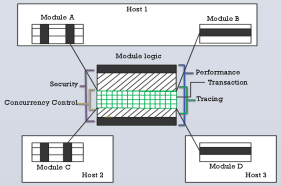

Limitations of AspectJ

- In AspectJ, joinpoints only deal with execution-flow context, e.g., the calling object, target object, and call stack.
- In AspectJ pointcuts can only express possible joinpoints in terms on basic program structures, like methods, constructors, fields, etc.
- AspectJ does not inherently handle application-level contexts, like a transaction, which may be tied to runtime objects used by multiple execution threads or processes.

Contributions

- A *Unified Model for Joinpoints in Distributed Transactions* (UMJDT) that that is rich enough to describe any transaction-related joinpoints and context information that make the most sense for DTPS's.

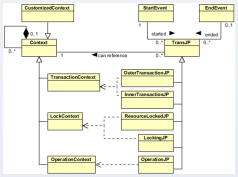

- A design and implementation of *TransJ*, including an implementation of UMJDT and JTA model.
- A toolkit consisting of reusable transaction aspects for common transaction-related crosscutting concerns, which verifies the correctness of UMJDT design. Such as performance measuring, logging, exception handling, audit trails, and tracing.
- A demonstration of the feasibility and utility of *TransJ* and a reusable aspect library through the implementation of DTAs and transaction aspects for those applications.
- An extension to a quality model to measure the effectiveness of *TransJ* in comparison with AspectJ.
- A preliminary experiment to test our hypotheses to discover whether *TransJ* can help achieve improved reuse without sacrificing performance when a system involved transaction-related crosscutting concerns.

TransJ Architecture

The core TransJ infrastructure layer enables aspect-oriented developers to treat transactions as first-class concepts into which AspectJ framework can weave crosscutting concerns in a modular way, i.e., transaction aspects.

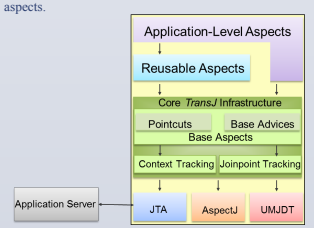

Transaction Events and Possible Joinpoints

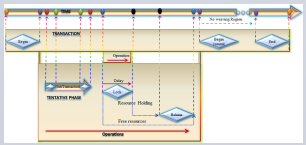

Initial Theoretical Comparison of TransJ to AspectJ

- Better Abstractions for Transactions.
- Improved the Reusability.
- Joinpoint Model Formalizes Transactional Joinpoints.
- Better Encapsulations and Localized Design Decisions.
- Improved Modularity and Obliviousness.
- Better Ways to Detangle Transaction Constructs from Core Application.
- Easy to Code Transaction Concerns.
- Conceptual Model Captures Transaction Context Information.
- More Structured Concerns for Transactions.

Design of TransJ Tool Set

- Transaction Joinpoints and Base Aspects within the Scope of the Transaction's Contexts

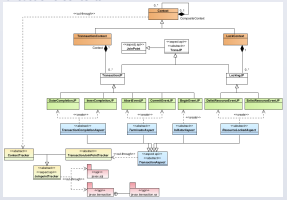

- Operation Joinpoints and Base Aspects within the Scope of the Operation's Contexts

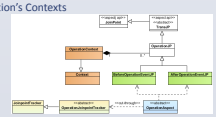

- Resource Joinpoints and Base Aspects within the Scope of the Lock's Contexts

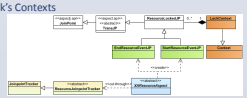

Extended Quality Model for Transactional Applications (EQMTA)

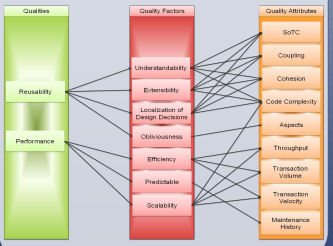

Measurement Metrics in EQMTA

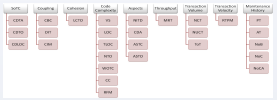

Hypotheses

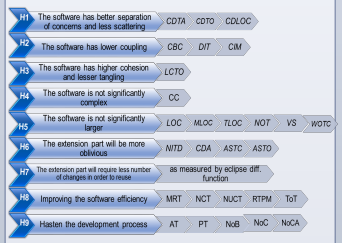

Experiment Methodology

Phase 1:

1. Passing the online Human Research Training course offered through the Collaborative *Institutional Training Initiative* (CITI).
2. Experimental Approval: Submitting IRB Application
3. Selection of Sample Applications: Developing three simple software applications and documenting their requirements, design, and implementation
4. Selection of Crosscutting Concerns from Sample Applications.
5. Sending invitation letters and recruiting up to 10 developers and organized them into two groups: group 1 & group 2
6. Assessing participants skill levels using questionnaires and surveys
7. Providing JTA, and JBoss Application Server training to developers in Group 1, and 2, and have them work through some practice applications.
8. Providing *AspectJ* training to Group 1 participants.
9. Providing *TransJ* training to developers in Group 2, and have them work through some practice applications.

Phase 2:

10. Asking participants to develop programs using given set of requirements
11. Asking the developers to complete a pre-implementation questionnaire, once they understand the code and documentation, provided them in Steps 7,8,9, and 10.
12. Asking the developers to develop the three crosscutting concerns, and then collecting their implementations using GitHub repository, and Box-file sharing.
13. Asking the developers to complete a post-questionnaire that helps to gather some additional information to measure quality metrics.
14. Measuring the quality metrics using EQMTA, collecting findings from the logs and prepost-questionnaires from Phase 1

Phase 3:

15. Giving enhancements (sample applications and crosscutting concerns) to all developers, have them review the crosscutting concerns, and then collect those revised implementations.
16. Asking the developers to complete a questionnaire that helps to gather some additional information to measure quality metrics.
17. Measuring Dependent Variables using Reuse/Performance Metrics
18. At the end; interpreting the results.

References

- Anas M. R. AlSobeh and Stephen W Clyde , Unified Conceptual Model for Joinpoints in Distributed Transactions. ICSEA 2014 : The Ninth International Conference on Software Engineering Advances. Nice France, IARIA, 2014. ISBN: 978-1-61208-367-4.
- Development reference guide for the JBossJTA implementation of the JTA API. http://docs.jboss.org/jbosstm/latest/guides/narayana-jta-development_guide/index.html

TransJ: Framework-Independent abstractions for Weaving Crosscutting Concerns into Distributed Transactions in AspectJ

Anas M.R AlSobeh, Stephen W Clyde

Utah State University

Abstract

Implementing crosscutting concerns for transactions is difficult, even using Aspect-Oriented Programming Languages (AOPL) such as AspectJ. Many of these challenges are because the context of transaction-related crosscutting concern is often a context consisting of loosely-coupled abstractions like dynamically generated identifiers, timestamps, and tentative value sets for distributed resources. Current AOPL do not provide joinpoints and pointcuts for weaving of advice into high-level abstractions, like transactions. Other challenges stem from essential complexity in the nature of the data, operations on the data, or the volume of data, and accidental complexity comes from the way that the problem is being solved even using common transaction frameworks. This paper describes an extension to AspectJ, called *TransJ*, with which developers can implement transaction-related concerns in cohesive and loosely coupled aspects. It also presents a preliminary experiment that we hope will provide evidence of improvement in reusability without sacrificing performance of applications requiring transactions.

Achieving Good Quality Software

Objective

An extension for AspectJ to weave transaction-related crosscutting concern into a DTPS in a modular and reusable way, while preserving the performance, core functionality, and obliviousness to those concerns.

Sample of Crosscutting Concerns

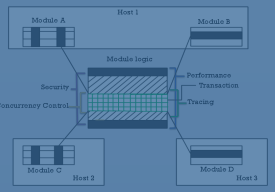

Limitations of AspectJ

- In AspectJ, joinpoints only deal with execution-flow context, e.g., the calling object, target object, and call stack.
- In AspectJ pointcuts can only express possible joinpoints in terms on basic program structures, like methods, constructors, fields, etc.
- AspectJ does not inherently handle application-level contexts, like a transaction, which may be tied to runtime objects used by multiple execution threads or processes.

Contributions

- A *Unified Model for Joinpoints in Distributed Transactions* (UMJDT) that that is rich enough to describe any transaction-related joinpoints and context information that make the most sense for DTPS's.

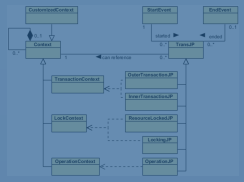

- A design and implementation of *TransJ*, including an implementation of UMJDT and JTA model.
- A toolkit consisting of reusable transaction aspects for common transaction-related crosscutting concerns, which verifies the correctness of UMJDT design. Such as performance measuring, logging, exception handling, audit trails, and tracing.
- A demonstration of the feasibility and utility of *TransJ* and a reusable aspect library through the implementation of DTAs and transaction aspects for those applications.
- An extension to a quality model to measure the effectiveness of *TransJ* in comparison with AspectJ.
- A preliminary experiment to test our hypotheses to discover whether *TransJ* can help achieve improved reuse without sacrificing performance when a system involved transaction-related crosscutting concerns.

TransJ Architecture

The core TransJ infrastructure layer enables aspect-oriented developers to treat transactions as first-class concepts into which AspectJ framework can weave crosscutting concerns in a modular way, i.e., transaction aspects.

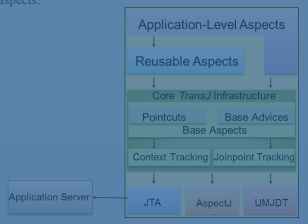

Transaction Events and Possible Joinpoints

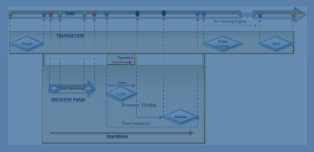

Initial Theoretical Comparison of TransJ to AspectJ

- Better Abstractions for Transactions.
- Improved the Reusability.
- Joinpoint Model Formalizes Transactional Joinpoints.
- Better Encapsulations and Localized Design Decisions.
- Improved Modularity and Obliviousness.
- Better Ways to Detangle Transaction Constructs from Core Application.
- Easy to Code Transaction Concerns.
- Conceptual Model Captures Transaction Context Information.
- More Structured Concerns for Transactions.

Design of TransJ Tool Set

- Transaction Joinpoints and Base Aspects within the Scope of the Transaction's Contexts

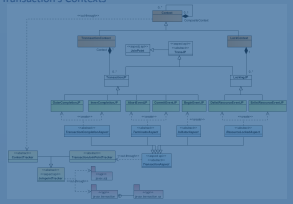

- Operation Joinpoints and Base Aspects within the Scope of the Operation's Contexts

- Resource Joinpoints and Base Aspects within the Scope of the Lock's Contexts

Extended Quality Model for Transactional Applications (EQMTA)

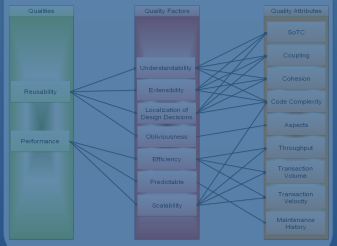

Measurement Metrics in EQMTA

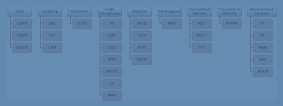

Hypotheses

Experiment Methodology

Phase 1:

1. Passing the online Human Research Training course offered through the *Collaborative Institutional Training Initiative* (CITI).
2. Experimental Approval: Submitting IRB Application
3. Selection of Sample Applications: Developing three simple software applications and documenting their requirements, design, and implementation
4. Selection of Crosscutting Concerns from Sample Applications.
5. Sending invitation letters and recruiting up to 10 developers and organized them into two groups: group 1 & group 2
6. Assessing participants skill levels using questionnaires and surveys
7. Providing JTA, and JBoss Application Server training to developers in Group 1, and 2, and have them work through some practice applications.
8. Providing *AspectJ* training to Group 1 participants.
9. Providing *TransJ* training to developers in Group 2 and have them work through some practice applications.

Phase 2:

10. Asking participants to develop programs using given set of requirements
11. Asking the developers to complete a pre-implementation questionnaire, once they understand the code and documentation, provided them in Steps 7,8,9, and 10.
12. Asking the developers to develop the three crosscutting concerns, and then collecting their implementations using GitHub repository, and Box-file sharing.
13. Asking the developers to complete a post-questionnaire that helps to gather some additional information to measure quality metrics.
14. Measuring the quality metrics using EQMTA, collecting findings from the logs and pre/post-questionnaires from Phase 1

Phase 3:

15. Giving enhancements (sample applications and crosscutting concerns) to all developers, have them review the crosscutting concerns, and then collect those revised implementations.
16. Asking the developers to complete a questionnaire that helps to gather some additional information to measure quality metrics.
17. Measuring Dependent Variables using Reuse/Performance Metrics
18. At the end; interpreting the results.

References

- Anas M. R. AlSobeh and Stephen W Clyde , Unified Conceptual Model for Joinpoints in Distributed Transactions. ICSEA 2014 : The Ninth International Conference on Software Engineering Advances. Nice France, IARIA, 2014. ISBN: 978-1-61208-367-4.
- Development reference guide for the JBossJTA implementation of the JTA API. http://docs.jboss.org/jbosstm/latest/guides/narayana-jta-development_guide/index.html

Experiment Methodology

Phase 1:

1. Passing the online Human Research Training course offered through the *Collaborative Institutional Training Initiative* (CITI).
2. Experimental Approval: Submitting IRB Application
3. Selection of Sample Applications: Developing three simple software applications and documenting their requirements, design, and implementation
4. Selection of Crosscutting Concerns from Sample Applications.
5. Sending invitation letters and recruiting up to 10 developers and organized them into two groups: group 1 & group 2
6. Assessing participants skill levels using questionnaires and surveys
7. Providing JTA, and JBoss Application Server training to developers in Group 1, and 2, and have them work through some practice applications.
8. Providing *AspectJ* training to Group 1 participants.
9. Providing *TransJ* training to developers in Group 2, and have them work through some practice applications.

Phase 2:

10. Asking participants to develop programs using given set of requirements
11. Asking the developers to complete a pre-implementation questionnaire, once they understand the code and documentation, provided them in Steps 7,8,9, and 10.
12. Asking the developers to develop the three crosscutting concerns, and then collecting their implementations using GitHub repository, and Box-file sharing.
13. Asking the developers to complete a post-questionnaire that helps to gather some additional information to measure quality metrics.
14. Measuring the quality metrics using EQMTA, collecting findings from the logs and pre/post-questionnaires from Phase 1

Phase 3:

15. Giving enhancements (sample applications and crosscutting concerns) to all developers, have them revise their implemented concerns, and then collect those revised implementations.
16. Asking the developers to complete a questionnaire that helps to gather some additional information to measure quality metrics.
17. Measuring Dependent Variables using Reuse/Performance Metrics
18. At the end; interpreting the results.

Experiment Methodology

Phase 1:

1. Passing the online Human Research Training course offered through the *Collaborative Institutional Training Initiative* (CITI).
2. Experimental Approval: Submitting IRB Application
3. Selection of Sample Applications: Developing three simple software applications and documenting their requirements, design, and implementation
4. Selection of Crosscutting Concerns from Sample Applications.
5. Sending invitation letters and recruiting up to 10 developers and organized them into two groups: group 1 & group 2
6. Assessing participants skill levels using questionnaires and surveys
7. Providing JTA, and JBoss Application Server training to developers in Group 1, and 2, and have them work through some practice applications.
8. Providing *AspectJ* training to Group 1 participants.
9. Providing *TransJ* training to developers in Group 2, and have them work through some practice applications.

SELF-ADVOCACY SKILLS

LSL Teacher Perceptions: Preschool through Third-Grade

Ariel Hendrix, B.S. (M.Ed. Candidate) & Lauri Nelson, Ph.D.

> "Children with hearing loss should learn that they have a right and responsibility to access the same educational and social experiences as their peers."

INTRODUCTION

Self-advocacy is an essential component of social-emotional skill development. For children who are deaf or hard of hearing (DHH), self-advocacy is considered especially critical, as the broader population is not always understanding of their needs. Regardless of the severity of loss, all children who are DHH need to demonstrate the ability to self-advocate across settings and may require additional support in developing these skills. Age-appropriate self-advocacy skills can and should be introduced within early intervention home-based programs and within the preschool classroom to establish the foundation for future growth and development.

METHODS

A self-advocacy ratings questionnaire for young children who are DHH was developed and distributed to preschool through third-grade listening & spoken language teachers.

Participants included 12 teachers who offered their perceptions on the self-advocacy skills of their students with hearing loss (n = 64).

Teachers completed both quantitative and qualitative survey components that revealed information on:

- student skill level in hearing technology management, social and academic self-advocacy skills and proactive listening.
- frequency and type of self-advocacy goals listed in student Individualized Education Programs (IEPs)
- self-advocacy skills taught within the classroom
- impact of self-advocacy skill level on academic and social/emotional development
- teacher recommendations for fostering self-advocacy skill development.

RESULTS

Teacher perceptions of skill level increased from preschool to kindergarten across all three self-advocacy priority areas (see inset).

Skill level was generally higher in areas of self-advocacy that required a lower level of skill. Skills that required higher levels of responsibility, greater expressive communication or interaction with others were identified as general areas of weakness.

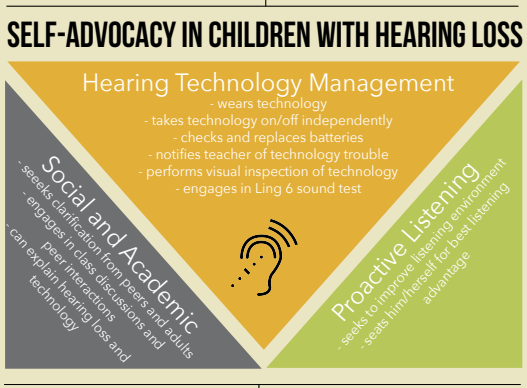

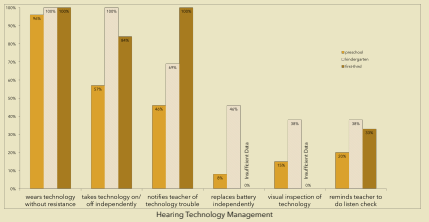

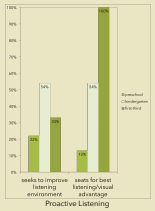

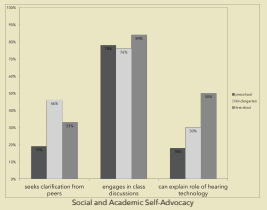

SKILL LEVELS

The following graphs indicate the frequency that each skill was mostly or always exhibited across age-groups:

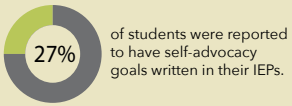

of students were reported to have self-advocacy goals written in their IEPs.

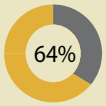

of students experienced negative effects on their academic and social/emotional development as a direct result of their self-advocacy skills.

For teachers who incorporated self-advocacy skills into their classroom instruction, a majority indicated that they focused on skills that required a lower level of responsibility or technical skill (e.g., consistent wearing of hearing technology, taking technology on/off), while very few identified more difficult skills as part of their curriculum (e.g., FM system responsibility, visual inspection of technology).

RECOMMENDATIONS

Children benefit when teachers foster age-appropriate self-advocacy skill development in their students across all self-advocacy priority areas and remain mindful that the level of self-advocacy skills attained in early childhood serve as a foundation for later success.

Children benefit when teachers utilize proper tools to identify areas of weakness in their students' level of self-advocacy skills and consciously incorporate them into IEP goal development and classroom instruction.

Utah State University

SELF-ADVOCACY SKILLS

LSL Teacher Perceptions: Preschool through Third-Grade

Ariel Hendrix, B.S. (M.Ed. Candidate) & Lauri Nelson, Ph.D.

> "Children with hearing loss should learn that they have a right and responsibility to access the same educational and social experiences as their peers."

INTRODUCTION

Self-advocacy is an essential component of social-emotional skill development. For children who are deaf or hard of hearing (DHH), self-advocacy is considered especially critical, as the broader population is not always understanding of their needs. Regardless of the severity of loss, all children who are DHH need to demonstrate the ability to self-advocate across settings and may require additional support in developing these skills. Age-appropriate self-advocacy skills can and should be introduced within early intervention home-based programs and within the preschool classroom to establish the foundation for future growth and development.

METHODS

A self-advocacy ratings questionnaire for young children who are DHH was developed and distributed to preschool through third-grade listening & spoken language teachers.

Participants included 12 teachers who offered their perceptions on the self-advocacy skills of their students with hearing loss (n = 64).

Teachers completed both quantitative and qualitative survey components that revealed information on:

- student skill level in hearing technology management, social and academic self-advocacy skills and proactive listening.
- frequency and type of self-advocacy goals listed in student Individualized Education Programs (IEPs)
- self-advocacy skills taught within the classroom
- impact of self-advocacy skill level on academic and social/emotional development
- teacher recommendations for fostering self-advocacy skill development.

RESULTS

Teacher perceptions of skill level increased from preschool to kindergarten across all three self-advocacy priority areas (see inset).

Skill level was generally higher in areas of self-advocacy that required a lower level of skill. Skills that required higher levels of responsibility, greater expressive communication or interaction with others were identified as general areas of weakness.

of students were reported to have self-advocacy goals written in their IEPs.

of students experienced negative effects on their academic and social/emotional development as a direct result of their self-advocacy skills.

For teachers who incorporated self-advocacy skills into their classroom instruction, a majority indicated that they focused on skills that required a lower level of responsibility or technical skill (e.g., consistent wearing of hearing technology, taking technology on/off), while very few identified more difficult skills as part of their curriculum (e.g., FM system responsibility, visual inspection of technology).

SKILL LEVELS

The following graphs indicate the frequency that each skill was mostly or always exhibited across age-groups:

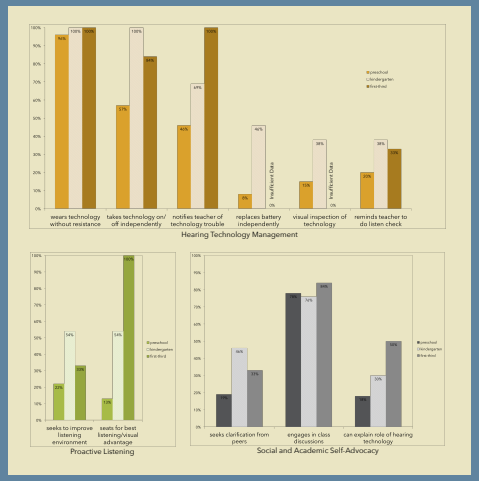

RECOMMENDATIONS

Children benefit when teachers foster age-appropriate self-advocacy skill development in their students across all self-advocacy priority areas and remain mindful that the level of self-advocacy skills attained in early childhood serve as a foundation for later success.

Children benefit when teachers utilize proper tools to identify areas of weakness in their students' level of self-advocacy skills and consciously incorporate them into IEP goal development and classroom instruction.

UtahState University

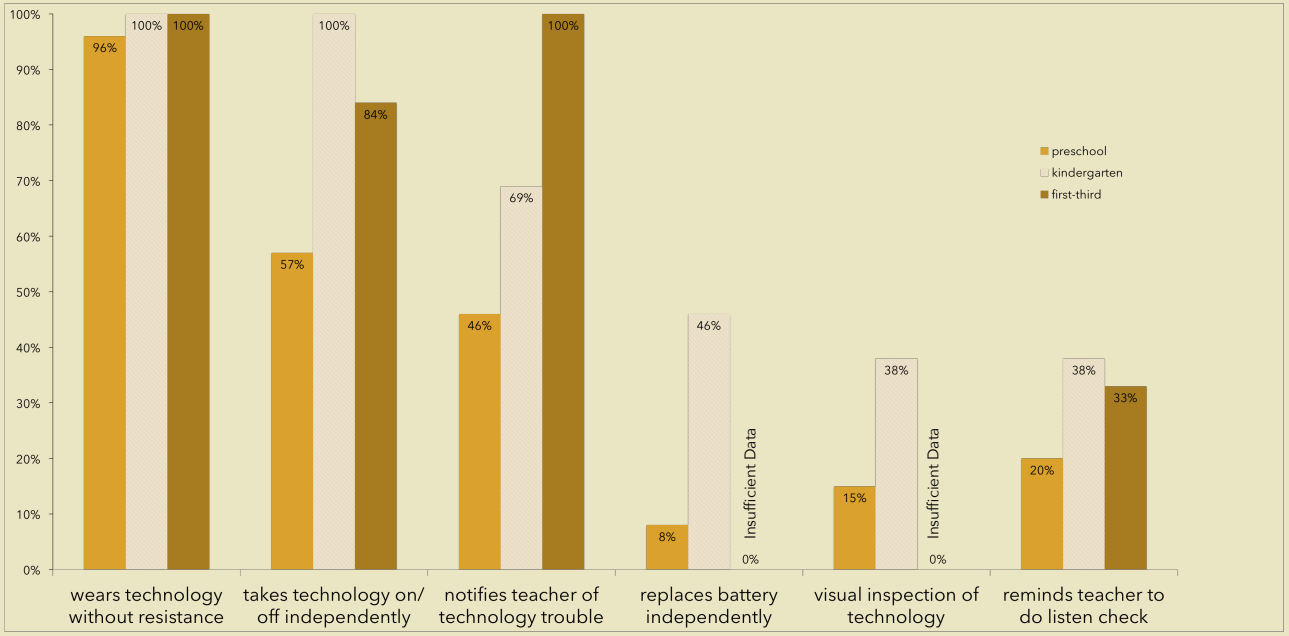

Hearing Technology Management

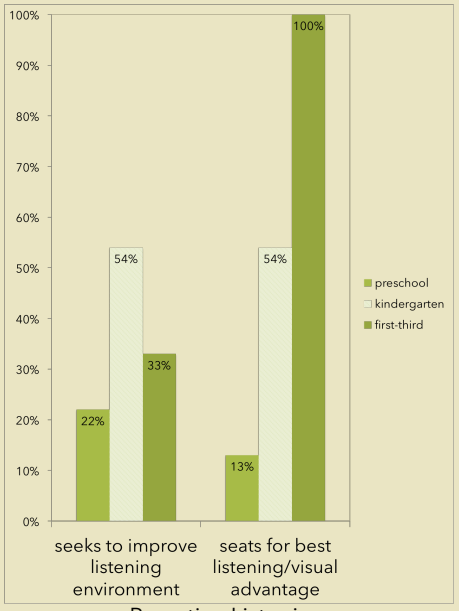

Proactive Listening

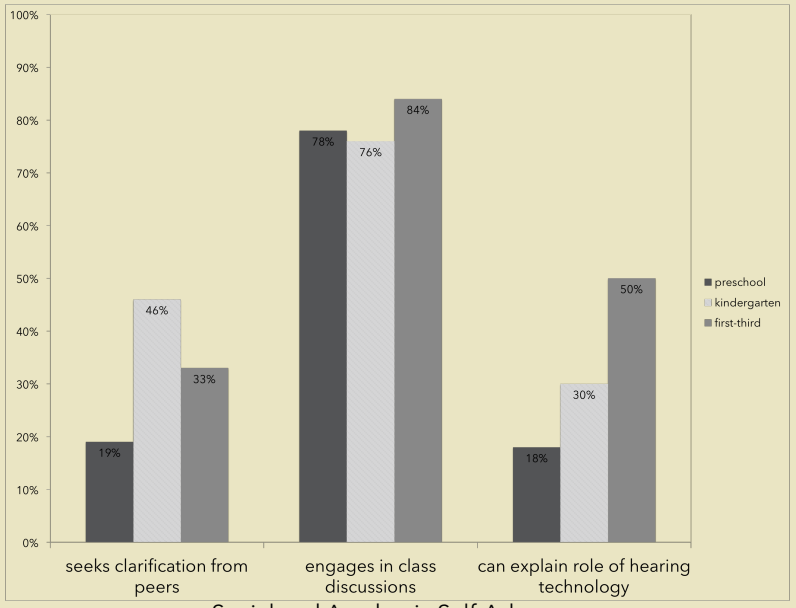

Social and Academic Self-Advocacy

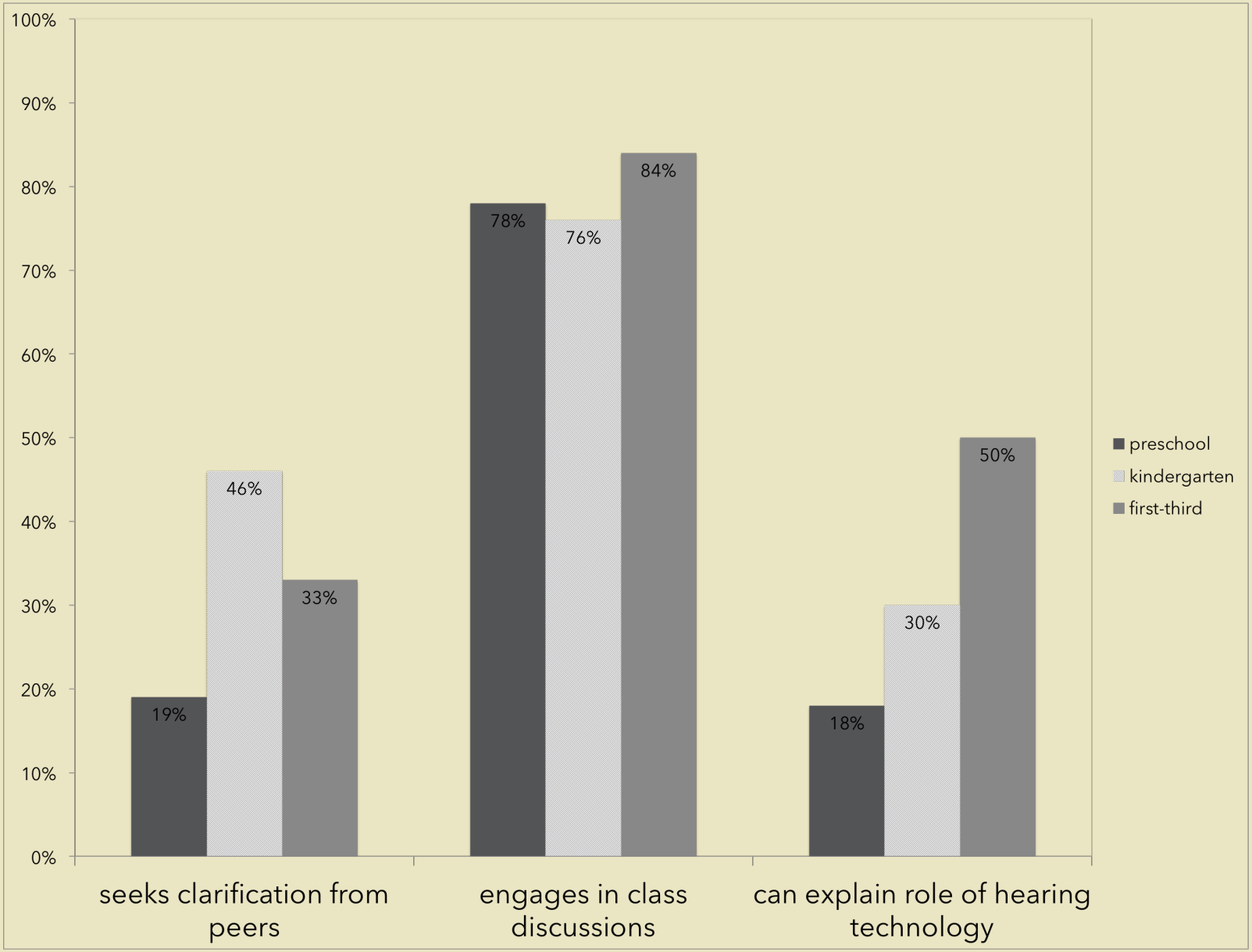

Social and Academic Self-Advocacy

Thermospheric Gravity Wave Characteristics Obtained Using the Poker Flat Incoherent Scatter Radar

Michael R. Negale[1], Kim Nielsen[2], Michael J. Taylor[1], and Michael J. Nicolls[3]
[1]Utah State University, [2]Utah Valley University, [3]SRI International

Introduction

Recent observational and modeling studies have revealed the importance of gravity waves propagating into in the thermospheric region (~110 – 400 km) as they contribute significantly to changes in both winds and temperatures [e.g. *Vadas and Fritts*, 2005]. The distributions and variability of these thermospheric gravity wave parameters are not yet known.

This presentation: details the process of obtaining wave parameters from the Poker Flat Incoherent Scatter Radar (PFISR) (based on a method developed by *Nicolls and Heinselman* [2007]) and presents preliminary wave characteristic distributions from August 2011 – April 2013.

- From the *Nicolls and Heinselman* [2007] case study:
  - horizontal wavelength of ~187 km
  - phase speed of ~140 m/s
  - period of ~22 min
  - propagating ~150° from north
- Propagation distributions from this analysis are compared to previous results of TIDs made using SuperDARN radars.
- Wavelengths vs. periods are compared with results obtained with a co-located mesospheric airglow imager.

PFISR

The Poker Flat Incoherent Scatter Radar (PFISR) facility, is operated at the Poker Flat Research Range (PFRR) (65° N, 147° W) near Fairbanks, Alaska. PFISR has operated since 2007 and uses a phased array technique enabling rapid pulse-to-pulse steering.

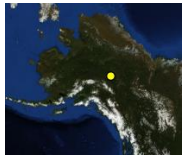

Location of PFRR in interior Alaska

PFISR situated at PFRR

Simultaneous observations from different parts of the ionosphere allows measurements of all relevant properties of the observed gravity waves, including their periods, horizontal and vertical wavelengths, horizontal phase speeds, and propagation directions [e.g. *Nicolls and Heinselman*, 2007] to be obtained. The wave parameters obtained for this analysis are extracted from electron density measurements.

PFISR Data Analysis

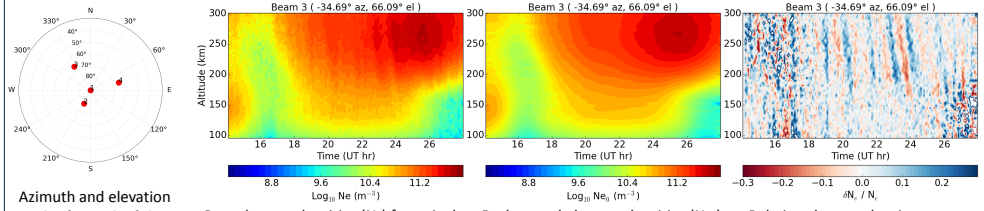

Azimuth and elevation angles for each of the 4 beams utilized by PFISR for observations on 25 October 2011.

Raw electron densities (N_e) for a single beam (#3) from ~14 – 30 UT over the altitude range ~100 – 300 km showing extensive gravity waves.

Background electron densities (N_{e0}) are estimated using a low-pass Butterworth filter at each altitude for each beam.

Relative electron density perturbations are calculated using $(N_e - N_{e0})/ N_{e0}$ to investigate the density fluctuations. The wave structure was strongest from ~18 – 30 UT and from ~160 – 300 km.

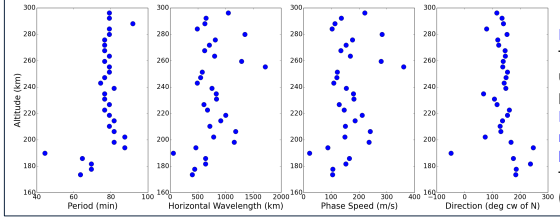

Method:
The dominant period of the wave and the wave vector are found using a complex cross-spectrum of the relative density perturbations at each altitude for each adjacent beam.
Left: Computed wave parameters vs. altitude for 25 October 2011, median observed period =79 min, horizontal wavelength =706 km horizontal phase speed =153 m/s, propagation azimuth ~140° N. These parameters are consistent with Medium Scale TIDs (MSTIDs). Note their consistency with altitude.

Results

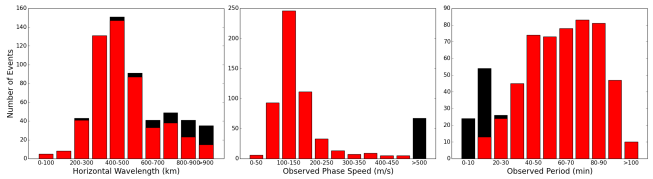

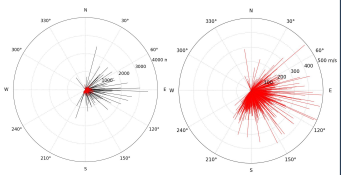

Summary results: In the standard form of histogram plots for the horizontal wavelength, observed phase speed, and period are shown. The data are plotted for the combined 2010 – 2013 observations, with a total of 595 events. Note a number of very high speed events (black). In order to compare with published results, we consider waves with phase speeds <500 m/s (red bars, 528).

- Wavelengths range from 200-600 km with a median of ~473 km.
- Phase speeds range from 60-250 m/s, with a median of ~137 m/s.
- Periods ranged from ~4 to > 100 min, with a median of ~60 min.

- The majority of the high phase speed (>500 m/s) waves (black lines) are propagating towards the east.
- The lower phase speed (< 500 m/s) MSTIDS (red lines) are seen to be propagating towards the east and southeast.

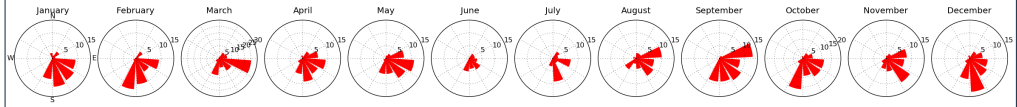

In order to investigate the monthly wave propagation distributions for the MSTIDs, we combined waves from 2010 – 2013 (total 33 months) into a single year and plotted them by month in 30° wide bins. For comparison, all data, except March and October, are plotted on the same scale.

- In each month the wave motions are predominantly southeastward.
- Variability in the wave propagation ranged from northeastward to southwestward.
- More waves were observed during the winter months with least occurrence in June and July.
- Remarkably no waves propagating in the northwest sector.

Discussion

Ishida et al. [2008] made observations of TIDs using two SuperDARN radars located in Alaska from December 2003 – February 2007. They observed 134 events almost all propagating southwards, but no northeast propagation.

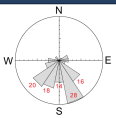

Ishida et al. [2008]

Frissell et al. [2014] made observations of mid-latitude TIDs using a SuperDARN radar located in Virginia (37° N) from June 2010 – May 2011. A majority of the TIDs observed were propagating towards the southeast at ~150°.

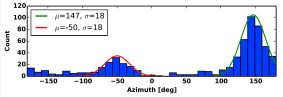

Frissell et al. [2014]

The propagation distribution of the TIDs obtained using PFISR show a majority of the waves to be propagating towards the southeast, similar to previous studies.

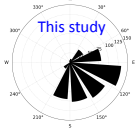

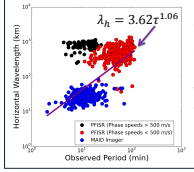

Wavelength vs. period from PFISR (black and red) and recent results from a co-located all-sky airglow imager (observations from 2011 – 2013) (blue) are shown along with a "global fit" (purple line) of optical, radar, and lidar measurements [e.g. *Reid*, 1986; *Taylor et al.* 1997]

Summary/Future Work

- Atmospheric gravity wave parameters were extracted from measured electron densities obtained from a number of different PFISR experiments run from August 2010 – April 2013.
- Over 500 MSTIDs were detected over the altitude range 100-300 km exhibiting well defined wave characteristics and dominant propagation directions towards the southeast.
- These propagation directions were found to be similar to other results obtained from SuperDARN radars in Alaska and Virginia.
- Wavelengths vs. periods from PFISR and a co-located all-sky airglow imager also agree will previous results.

Future work:

- Investigate wave characteristic as a function of altitude in 50 km altitude ranges from 100 – 300 km.
- Use spectral analysis to investigate other wave contributions.

References

- Frissell, N.A., J.B.H. Baker, J.M. Ruohoniemi, A.J. Gerrard, E.S. Miller, J.P. Marini, M.
- L. West, and W.A. Bristow (2014), Climatology of medium-scale traveling ionospheric disturbances observed by the midlatitude Balckstone SuperDARN radar, *J. Geophys. Res., 119*, 7679-7697, doi:10.1002/2014JA019870.
- Fritts, D.C. and M. J. Alexander (2003), Gravity wave dynamics and effects in the middle atmosphere, *Rev. Geophys. 41*, 1003, doi:10.1029/2001RG00106.
- Ishida, T., K. Hosokawa, T. Shibata, S. Suzuki, N. Nishitani, and T. Ogawa (2008), SuperDARN observations of daytime MSTIDs in the auroral and mid-latitudes: Possibly of long-distance propagation, *Geophys. Res. Lett., 35*, L13102, doi:10.1029/2008GL034623.
- Nicolls, M. J. and C. J. Heinselman (2007), Three-dimensional measurements of traveling ionospheric disturbances with the Poker Flat Incoherent Scatter Radar, *Geophys. Res. Lett., 34*, L21104, doi:10.1029/2007GL031506.
- Ried, I. M. (1986), Gravity wave motions in the upper middle atmosphere (60-110 km), *J. Atmos. Terr. Phys. 48* (11-12), 1057.
- Taylor, M. J., W. R. Pendleton, S. Clark, H. Takahashi, D. Gobbi, R. A. Goldberg (1997), Image measurements of short-period gravity waves at equatorial latitudes, *J. Geophys. Res. 102*, D22.
- Vadas, S. and D. C. Fritts (2005), Thermospheric responses to gravity waves: Influences of increasing viscosity and thermal diffusivity, *J. Geophys. Res., 110*, D15103, doi:10.1029/2004JD005574.

Acknowledgments

This project was funded by the National Science Foundation (NSF), Office of Polar Programs Grant OPP-1023265 titled "Collaborative Research: an Investigation of Wave Dynamics in the Arctic Mesosphere and Coupling Between the Lower and Upper Polar Atmosphere" (PI: K. Nielsen, UVU) Michael R. Negale is also supported by the NSF Graduate Research Fellowship under Grant #1147384.

Thermospheric Gravity Wave Characteristics Obtained Using the Poker Flat Incoherent Scatter Radar

Michael R. Negale[1], Kim Nielsen[2], Michael J. Taylor[1], and Michael J. Nicolls[3]
[1]Utah State University, [2]Utah Valley University, [3]SRI International

Introduction

Recent observational and modeling studies have revealed the importance of gravity waves propagating into in the thermospheric region (~110 – 400 km) as they contribute significantly to changes in both winds and temperatures [e.g. *Vadas and Fritts*, 2005]. The distributions and variability of these thermospheric gravity wave parameters are not yet known.

This presentation: details the process of obtaining wave parameters from the Poker Flat Incoherent Scatter Radar (PFISR) (based on a method developed by *Nicolls and Heinselman* [2007]) and presents preliminary wave characteristic distributions from August 2011 – April 2013.

- From the *Nicolls and Heinselman* [2007] case study:
  - horizontal wavelength of ~187 km
  - phase speed of ~140 m/s
  - period of ~22 min
  - propagating ~150° from north
- Propagation distributions from this analysis are compared to previous results of TIDs made using SuperDARN radars.
- Wavelengths vs. periods are compared with results obtained with a co-located mesospheric airglow imager.

PFISR

The Poker Flat Incoherent Scatter Radar (PFISR) facility, is operated at the Poker Flat Research Range (PFRR) (65° N, 147° W) near Fairbanks, Alaska. PFISR has operated since 2007 and uses a phased array technique enabling rapid pulse-to-pulse steering.

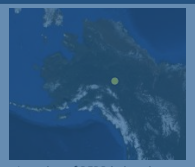

Location of PFRR in interior Alaska

PFISR situated at PFRR

Simultaneous observations from different parts of the ionosphere allows measurements of all relevant properties of the observed gravity waves, including their periods, horizontal and vertical wavelengths, horizontal phase speeds, and propagation directions [e.g. *Nicolls and Heinselman*, 2007] to be obtained. The wave parameters obtained for this analysis are extracted from electron density measurements.

PFISR Data Analysis

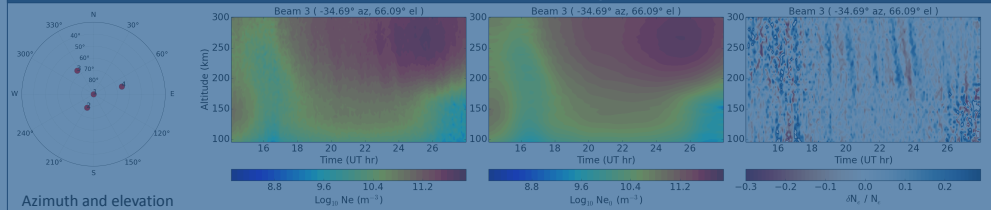

Azimuth and elevation angles for each of the 4 beams utilized by PFISR for observations on 25 October 2011.

Raw electron densities (N_e) for a single beam (#3) from ~14 – 30 UT over the altitude range ~100 – 300 km showing extensive gravity waves.

Background electron densities (N_{e0}) are estimated using a low-pass Butterworth filter at each altitude for each beam.

Relative electron density perturbations are calculated using $(N_e - N_{e0})/ N_{e0}$ to investigate the density fluctuations. The wave structure was strongest from ~18 – 30 UT and from ~160 – 300 km.

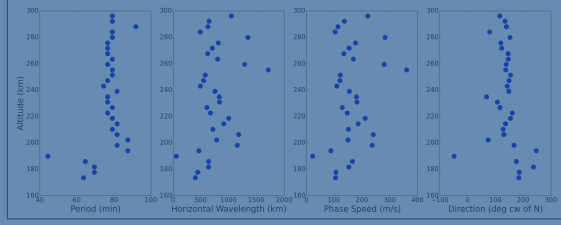

Method:
The dominant period of the wave and the wave vector are found using a complex cross-spectrum of the relative density perturbations at each altitude for each adjacent beam.
Left: Computed wave parameters vs. altitude for 25 October 2011, median observed period =79 min, horizontal wavelength =706 km horizontal phase speed =153 m/s, propagation azimuth ~140° N. These parameters are consistent with Medium Scale TIDs (MSTIDs). Note their consistency with altitude.

Results

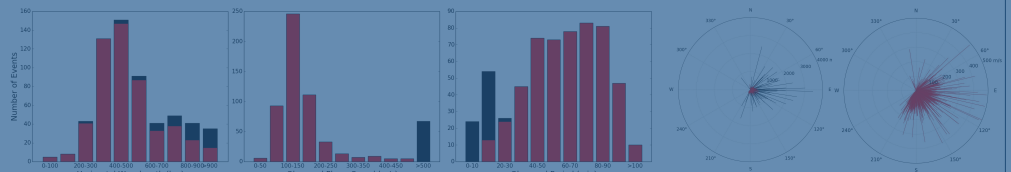

Summary results: In the standard form of histogram plots for the horizontal wavelength, observed phase speed, and period are shown. The data are plotted for the combined 2010 – 2013 observations, with a total of 595 events. Note a number of very high speed events (black). In order to compare with published results, we consider waves with phase speeds <500 m/s (red bars, 528).

- Wavelengths range from 200-600 km with a median of ~473 km.
- Phase speeds range from 60-250 m/s, with a median of ~137 m/s.
- Periods ranged from ~4 to > 100 min, with a median of ~60 min.

- The majority of the high phase speed (>500 m/s) waves (black lines) are propagating towards the east.
- The lower phase speed (< 500 m/s) MSTIDS (red lines) are seen to be propagating towards the east and southeast.

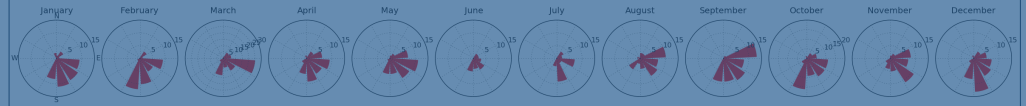

In order to investigate the monthly wave propagation distributions for the MSTIDs, we combined waves from 2010 – 2013 (total 33 months) into a single year and plotted them by month in 30° wide bins. For comparison, all data, except March and October, are plotted on the same scale.

- In each month the wave motions are predominantly southeastward.
- Variability in the wave propagation ranged from northeastward to southwestward.
- More waves were observed during the winter months with least occurrence in June and July.
- Remarkably no waves propagating in the northwest sector.

Discussion

Ishida et al. [2008] made observations of TIDs using two SuperDARN radars located in Alaska from December 2003 – February 2007. They observed 134 events almost all propagating southwards, but no northeast propagation.

Ishida et al. [2008]

Frissell et al. [2014] made observations of mid-latitude TIDs using a SuperDARN radar located in Virginia (37° N) from June 2010 – May 2011. A majority of the TIDs observed were propagating towards the southeast at ~150°.

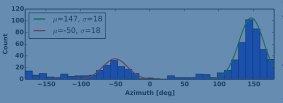

Frissell et al. [2014]

The propagation distribution of the TIDs obtained using PFISR show a majority of the waves to be propagating towards the southeast, similar to previous studies.

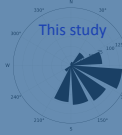

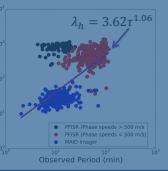

Wavelength vs. period from PFISR (black and red) and recent results from a co-located all-sky airglow imager (observations from 2011 – 2013) (blue) are shown along with a "global fit" (purple line) of optical, radar, and lidar measurements [e.g. *Reid*, 1986; *Taylor et al.* 1997]

Summary/Future Work

- Atmospheric gravity wave parameters were extracted from measured electron densities obtained from a number of different PFISR experiments run from August 2010 – April 2013.
- Over 500 MSTIDs were detected over the altitude range 100-300 km exhibiting well defined wave characteristics and dominant propagation directions towards the southeast.
- These propagation directions were found to be similar to other results obtained from SuperDARN radars in Alaska and Virginia.
- Wavelengths vs. periods from PFISR and a co-located all-sky airglow imager also agree will previous results.

Future work:

- Investigate wave characteristic as a function of altitude in 50 km altitude ranges from 100 – 300 km.
- Use spectral analysis to investigate other wave contributions.

References

- Frissell, N.A., J.B.H. Baker, J.M. Ruohoniemi, A.J. Gerrard, E.S. Miller, J.P. Marini, M.
- L. West, and W.A. Bristow (2014), Climatology of medium-scale traveling ionospheric disturbances observed by the midlatitude Balckstone SuperDARN radar, *J. Geophys. Res., 119*, 7679-7697, doi:10.1002/2014JA019870.
- Fritts, D.C. and M. J. Alexander (2003), Gravity wave dynamics and effects in the middle atmosphere, *Rev. Geophys. 41*, 1003, doi:10.1029/2001RG00106.
- Ishida, T., K. Hosokawa, T. Shibata, S. Suzuki, N. Nishitani, and T. Ogawa (2008), SuperDARN observations of daytime MSTIDs in the auroral and mid-latitudes: Possibly of long-distance propagation, *Geophys. Res. Lett., 35*, L13102, doi:10.1029/2008GL034623.
- Nicolls, M. J. and C. J. Heinselman (2007), Three-dimensional measurements of traveling ionospheric disturbances with the Poker Flat Incoherent Scatter Radar, *Geophys. Res. Lett., 34*, L21104, doi:10.1029/2007GL031506.
- Ried, I. M. (1986), Gravity wave motions in the upper middle atmosphere (60-110 km), *J. Atmos. Terr. Phys. 48* (11-12), 1057.
- Taylor, M. J., W. R. Pendleton, S. Clark, H. Takahashi, D. Gobbi, R. A. Goldberg (1997), Image measurements of short-period gravity waves at equatorial latitudes, *J. Geophys. Res. 102*, D22.
- Vadas, S. and D. C. Fritts (2005), Thermospheric responses to gravity waves: Influences of increasing viscosity and thermal diffusivity, *J. Geophys. Res., 110*, D15103, doi:10.1029/2004JD005574.

Acknowledgments

This project was funded by the National Science Foundation (NSF), Office of Polar Programs Grant OPP-1023265 titled "Collaborative Research: an Investigation of Wave Dynamics in the Arctic Mesosphere and Coupling Between the Lower and Upper Polar Atmosphere" (PI: K. Nielsen, UVU) Michael R. Negale is also supported by the NSF Graduate Research Fellowship under Grant #1147384.

Thermospheric Gravity Wave Characteristics Obtained Using the Poker Flat Incoherent Scatter Radar

Michael R. Negale[1], Kim Nielsen[2], Michael J. Taylor[1], and Michael J. Nicolls[3]
[1]Utah State University, [2]Utah Valley University, [3]SRI International

Introduction

Recent observational and modeling studies have revealed the importance of gravity waves propagating into in the thermospheric region (~110 – 400 km) as they contribute significantly to changes in both winds and temperatures [e.g. *Vadas and Fritts*, 2005]. The distributions and variability of these thermospheric gravity wave parameters are not yet known.

This presentation: details the process of obtaining wave parameters from the Poker Flat Incoherent Scatter Radar (PFISR) (based on a method developed by *Nicolls and Heinselman* [2007]) and presents preliminary wave characteristic distributions from August 2011 – April 2013.

- From the *Nicolls and Heinselman* [2007] case study:
  - horizontal wavelength of ~187 km
  - phase speed of ~140 m/s
  - period of ~22 min
  - propagating ~150° from north
- Propagation distributions from this analysis are compared to previous results of TIDs made using SuperDARN radars.
- Wavelengths vs. periods are compared with results obtained with a co-located mesospheric airglow imager.

PFISR

The Poker Flat Incoherent Scatter Radar (PFISR) facility, is operated at the Poker Flat Research Range (PFRR) (65° N, 147° W) near Fairbanks, Alaska. PFISR has operated since 2007 and uses a phased array technique enabling rapid pulse-to-pulse steering.

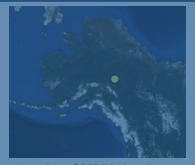

Location of PFRR in interior Alaska

PFISR situated at PFRR

Simultaneous observations from different parts of the ionosphere allows measurements of all relevant properties of the observed gravity waves, including their periods, horizontal and vertical wavelengths, horizontal phase speeds, and propagation directions [e.g. *Nicolls and Heinselman*, 2007] to be obtained. The wave parameters obtained for this analysis are extracted from electron density measurements.

PFISR Data Analysis

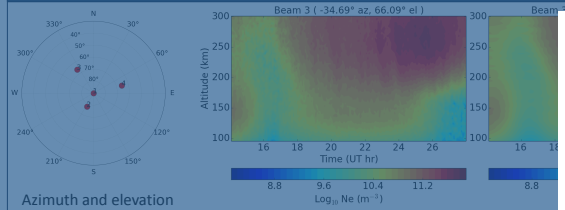

Azimuth and elevation angles for each of the 4 beams utilized by PFISR for observations on 25 October 2011.

Raw electron densities (N_e) for a single beam (#3) from ~14 – 30 UT over the altitude range ~100 – 300 km showing extensive gravity waves.

Backgroun
are estimat
Butterwort
each beam

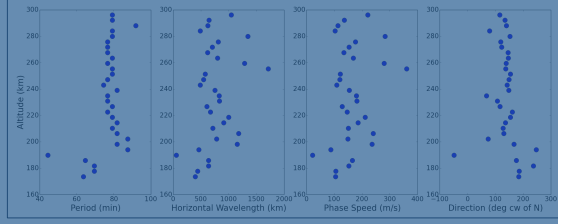

Results

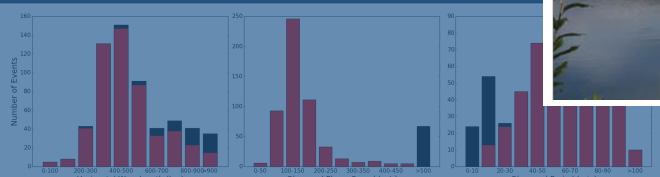

Summary results: In the standard form of histogram plots for the horizontal wavelength, observed phase speed, and period are shown. The data are plotted for the combined 2010 – 2013 observations, with a total of 595 events. Note a number of very high speed events (black). In order to compare with published results, we consider waves with phase speeds <500 m/s (red bars, 528).

- Wavelengths range from 200-600 km with a median of ~473 km.
- Phase speeds range from 60-250 m/s, with a median of ~137 m/s.
- Periods ranged from ~4 to > 100 min, with a median of ~60 min.

- The majority of the high phase speed (>500 m/s) waves (black lines) are propagating towards the east.
- The lower phase speed (< 500 m/s) MSTIDS (red lines) are seen to be propagating towards the east and southeast.

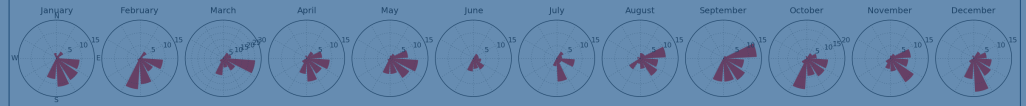

In order to investigate the monthly wave propagation distributions for the MSTIDs, we combined waves from 2010 – 2013 (total 33 months) into a single year and plotted them by month in 30° wide bins. For comparison, all data, except March and October, are plotted on the same scale.

- In each month the wave motions are predominantly southeastward.
- Variability in the wave propagation ranged from northeastward to southwestward.
- More waves were observed during the winter months with least occurrence in June and July.
- Remarkably no waves propagating in the northwest sector.

Discussion

Atmospheric gravity wave parameters were extracted from measured electron densities obtained from a number of different PFISR experiments run from August 2010 – April 2013.

- Over 500 MSTIDs were detected over the altitude range 100-300 km exhibiting well defined wave characteristics and dominant propagation directions towards the southeast.
- These propagation directions were found to be similar to other results obtained from SuperDARN radars in Alaska and Virginia.
- Wavelengths vs. periods from PFISR and a co-located all-sky airglow imager also agree will previous results.

Future work:

- Investigate wave characteristic as a function of altitude in 50 km altitude ranges from 100 – 300 km.
- Use spectral analysis to investigate other wave contributions.

References

- Frissell, N.A., J.B.H. Baker, J.M. Ruohoniemi, A.J. Gerrard, E.S. Miller, J.P. Marini, M.
- L. West, and W.A. Bristow (2014), Climatology of medium-scale traveling ionospheric disturbances observed by the midlatitude Balckstone SuperDARN radar, *J. Geophys. Res., 119*, 7679-7697, doi:10.1002/2014JA019870.
- Fritts, D.C. and M. J. Alexander (2003), Gravity wave dynamics and effects in the middle atmosphere, *Rev. Geophys. 41*, 1003, doi:10.1029/2001RG00106.
- Ishida, T., K. Hosokawa, T. Shibata, S. Suzuki, N. Nishitani, and T. Ogawa (2008), SuperDARN observations of daytime MSTIDs in the auroral and mid-latitudes: Possibly of long-distance propagation, *Geophys. Res. Lett., 35*, L13102, doi:10.1029/2008GL034623.
- Nicolls, M. J. and C. J. Heinselman (2007), Three-dimensional measurements of traveling ionospheric disturbances with the Poker Flat Incoherent Scatter Radar, *Geophys. Res. Lett., 34*, L21104, doi:10.1029/2007GL031506.
- Ried, I. M. (1986), Gravity wave motions in the upper middle atmosphere (60-110 km), *J. Atmos. Terr. Phys. 48* (11-12), 1057.
- Taylor, M. J., W. R. Pendleton, S. Clark, H. Takahashi, D. Gobbi, R. A. Goldberg (1997), Image measurements of short-period gravity waves at equatorial latitudes, *J. Geophys. Res. 102*, D22.
- Vadas, S. and D. C. Fritts (2005), Thermospheric responses to gravity waves: Influences of increasing viscosity and thermal diffusivity, *J. Geophys. Res., 110*, D15103, doi:10.1029/2004JD005574.

Acknowledgments

This project was funded by the National Science Foundation (NSF), Office of Polar Programs Grant OPP-1023265 titled "Collaborative Research: an Investigation of Wave Dynamics in the Arctic Mesosphere and Coupling Between the Lower and Upper Polar Atmosphere" (PI: K. Nielsen, UVU) Michael R. Negale is also supported by the NSF Graduate Research Fellowship under Grant #1147384.

Thermospheric Gravity Wave Characteristics Obtained Using the Poker Flat Incoherent Scatter Radar

Michael R. Negale[1], Kim Nielsen[2], Michael J. Taylor[1], and Michael J. Nicolls[3]
[1]Utah State University, [2]Utah Valley University, [3]SRI International

Introduction

Recent observational and modeling studies have revealed the importance of gravity waves propagating into in the thermospheric region (~110 – 400 km) as they contribute significantly to changes in both winds and temperatures [e.g. *Vadas and Fritts*, 2005]. The distributions and variability of these thermospheric gravity wave parameters are not yet known.

This presentation: details the process of obtaining wave parameters from the Poker Flat Incoherent Scatter Radar (PFISR) (based on a method developed by *Nicolls and Heinselman* [2007]) and presents preliminary wave characteristic distributions from August 2011 – April 2013.

- From the *Nicolls and Heinselman* [2007] case study:
  - horizontal wavelength of ~187 km
  - phase speed of ~140 m/s
  - period of ~22 min
  - propagating ~150° from north
- Propagation distributions from this analysis are compared to previous results of TIDs made using SuperDARN radars.
- Wavelengths vs. periods are compared with results obtained with a co-located mesospheric airglow imager.

PFISR

The Poker Flat Incoherent Scatter Radar (PFISR) facility, is operated at the Poker Flat Research Range (PFRR) (65° N, 147° W) near Fairbanks, Alaska. PFISR has operated since 2007 and uses a phased array technique enabling rapid pulse-to-pulse steering.

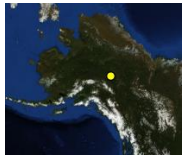

Location of PFRR in interior Alaska

PFISR situated at PFRR

Simultaneous observations from different parts of the ionosphere allows measurements of all relevant properties of the observed gravity waves, including their periods, horizontal and vertical wavelengths, horizontal phase speeds, and propagation directions [e.g. *Nicolls and Heinselman*, 2007] to be obtained. The wave parameters obtained for this analysis are extracted from electron density measurements.

PFISR Data Analysis

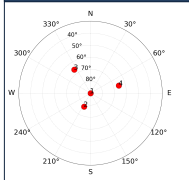

Azimuth and elevation angles for each of the 4 beams utilized by PFISR for observations on 25 October 2011.

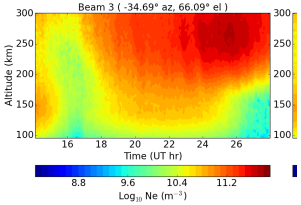

Raw electron densities (N_e) for a single beam (#3) from ~14 – 30 UT over the altitude range ~100 – 300 km showing extensive gravity waves.

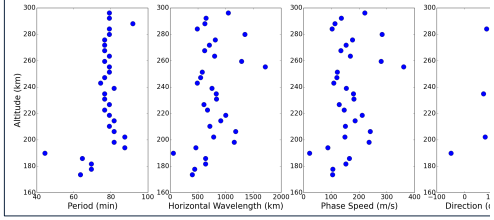

Re

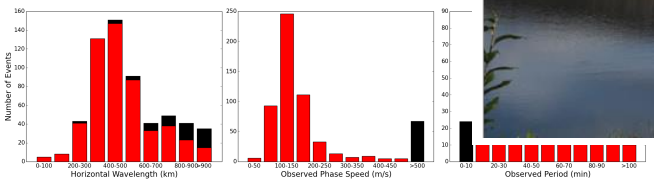

Summary results: In the standard form of histogram plots for the horizontal wavelength, observed phase speed, and period are shown. The data are plotted for the combined 2010 – 2013 observations, with a total of 595 events. Note a number of very high speed events (black). In order to compare with published results, we consider waves with phase speeds <500 m/s (red bars, 528).

- Wavelengths range from 200-600 km with a median of ~473 km.
- Phase speeds range from 60-250 m/s, with a median of ~137 m/s.
- Periods ranged from ~4 to > 100 min, with a median of ~60 min.

- The majority of the high phase speed (>500 m/s) waves (black lines) are propagating towards the east.
- The lower phase speed (< 500 m/s) MSTIDS (red lines) are seen to be propagating towards the east and southeast.

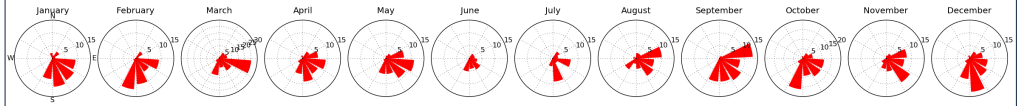

In order to investigate the monthly wave propagation distributions for the MSTIDs, we combined waves from 2010 – 2013 (total 33 months) into a single year and plotted them by month in 30° wide bins. For comparison, all data, except March and October, are plotted on the same scale.

- In each month the wave motions are predominantly southeastward.
- Variability in the wave propagation ranged from northeastward to southwestward.
- More waves were observed during the winter months with least occurrence in June and July.
- Remarkably no waves propagating in the northwest sector.

Discussion

- Over 500 MSTIDs were detected over the altitude range 100-300 km exhibiting well defined wave characteristics and dominant propagation directions towards the southeast.
- These propagation directions were found to be similar to other results obtained from SuperDARN radars in Alaska and Virginia.
- Wavelengths vs. periods from PFISR and a co-located all-sky airglow imager also agree will previous results.

Future work:

- Investigate wave characteristic as a function of altitude in 50 km altitude ranges from 100 – 300 km.
- Use spectral analysis to investigate other wave contributions.

References

- Frissell, N.A., J.B.H. Baker, J.M. Ruohoniemi, A.J. Gerrard, E.S. Miller, J.P. Marini, M.
- L. West, and W.A. Bristow (2014), Climatology of medium-scale traveling ionospheric disturbances observed by the midlatitude Balckstone SuperDARN radar, *J. Geophys. Res., 119*, 7679-7697, doi:10.1002/2014JA019870.
- Fritts, D.C. and M. J. Alexander (2003), Gravity wave dynamics and effects in the middle atmosphere, *Rev. Geophys. 41*, 1003, doi:10.1029/2001RG00106.
- Ishida, T., K. Hosokawa, T. Shibata, S. Suzuki, N. Nishitani, and T. Ogawa (2008), SuperDARN observations of daytime MSTIDs in the auroral and mid-latitudes: Possibly of long-distance propagation, *Geophys. Res. Lett., 35*, L13102, doi:10.1029/2008GL034623.
- Nicolls, M. J. and C. J. Heinselman (2007), Three-dimensional measurements of traveling ionospheric disturbances with the Poker Flat Incoherent Scatter Radar, *Geophys. Res. Lett., 34*, L21104, doi:10.1029/2007GL031506.
- Ried, I. M. (1986), Gravity wave motions in the upper middle atmosphere (60-110 km), *J. Atmos. Terr. Phys. 48* (11-12), 1057.
- Taylor, M. J., W. R. Pendleton, S. Clark, H. Takahashi, D. Gobbi, R. A. Goldberg (1997), Image measurements of short-period gravity waves at equatorial latitudes, *J. Geophys. Res. 102*, D22.
- Vadas, S. and D. C. Fritts (2005), Thermospheric responses to gravity waves: Influences of increasing viscosity and thermal diffusivity, *J. Geophys. Res., 110*, D15103, doi:10.1029/2004JD005574.

Acknowledgments

This project was funded by the National Science Foundation (NSF), Office of Polar Programs Grant OPP-1023265 titled "Collaborative Research: an Investigation of Wave Dynamics in the Arctic Mesosphere and Coupling Between the Lower and Upper Polar Atmosphere" (PI: K. Nielsen, UVU) Michael R. Negale is also supported by the NSF Graduate Research Fellowship under Grant #1147384.

Thermospheric Gravity Wave Characteristics Obtained Using the Poker Flat Incoherent Scatter Radar

Michael R. Negale[1], Kim Nielsen[2], Michael J. Taylor[1], and Michael J. Nicolls[3]
[1]Utah State University, [2]Utah Valley University, [3]SRI International

Introduction

Recent observational and modeling studies have revealed the importance of gravity waves propagating into in the thermospheric region (~110 – 400 km) as they contribute significantly to changes in both winds and temperatures [e.g. *Vadas and Fritts*, 2005]. The distributions and variability of these thermospheric gravity wave parameters are not yet known.

This presentation: details the process of obtaining wave parameters from the Poker Flat Incoherent Scatter Radar (PFISR) (based on a method developed by *Nicolls and Heinselman* [2007]) and presents preliminary wave characteristic distributions from August 2011 – April 2013.

- From the *Nicolls and Heinselman* [2007] case study:
  - horizontal wavelength of ~187 km
  - phase speed of ~140 m/s
  - period of ~22 min
  - propagating ~150° from north
- Propagation distributions from this analysis are compared to previous results of TIDs made using SuperDARN radars.
- Wavelengths vs. periods are compared with results obtained with a co-located mesospheric airglow imager.

PFISR

The Poker Flat Incoherent Scatter Radar (PFISR) facility, is operated at the Poker Flat Research Range (PFRR) (65° N, 147° W) near Fairbanks, Alaska. PFISR has operated since 2007 and uses a phased array technique enabling rapid pulse-to-pulse steering.

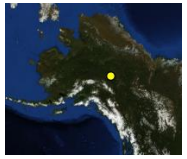

Location of PFRR in interior Alaska

PFISR situated at PFRR

Simultaneous observations from different parts of the ionosphere allows measurements of all relevant properties of the observed gravity waves, including their periods, horizontal and vertical wavelengths, horizontal phase speeds, and propagation directions [e.g. *Nicolls and Heinselman*, 2007] to be obtained. The wave parameters obtained for this analysis are extracted from electron density measurements.

PFISR Data Analysis

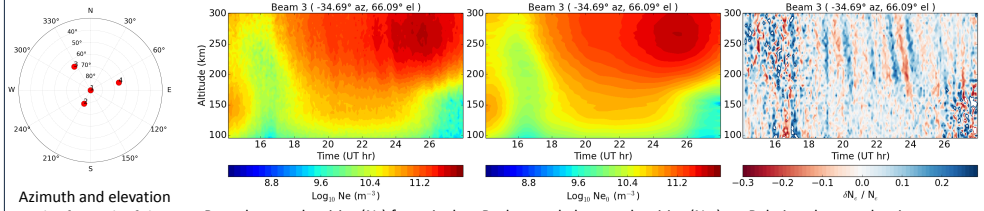

Azimuth and elevation angles for each of the 4 beams utilized by PFISR for observations on 25 October 2011.

Raw electron densities (N_e) for a single beam (#3) from ~14 – 30 UT over the altitude range ~100 – 300 km showing extensive gravity waves.

Background electron densities (N_{e0}) are estimated using a low-pass Butterworth filter at each altitude for each beam.

Relative electron density perturbations are calculated using $(N_e - N_{e0})/ N_{e0}$ to investigate the density fluctuations. The wave structure was strongest from ~18 – 30 UT and from ~160 – 300 km.

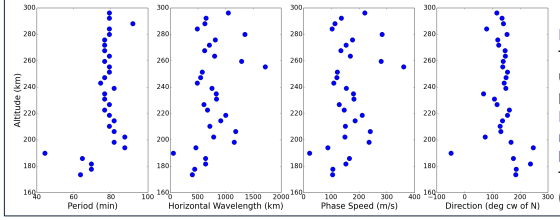

Method:
The dominant period of the wave and the wave vector are found using a complex cross-spectrum of the relative density perturbations at each altitude for each adjacent beam.
Left: Computed wave parameters vs. altitude for 25 October 2011, median observed period =79 min, horizontal wavelength =706 km horizontal phase speed =153 m/s, propagation azimuth ~140° N. These parameters are consistent with Medium Scale TIDs (MSTIDs). Note their consistency with altitude.

Results

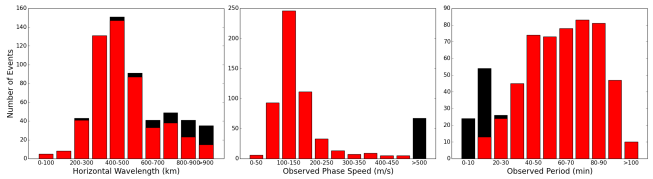

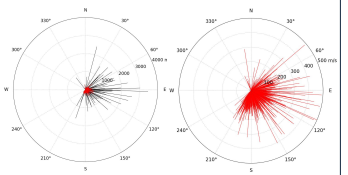

Summary results: In the standard form of histogram plots for the horizontal wavelength, observed phase speed, and period are shown. The data are plotted for the combined 2010 – 2013 observations, with a total of 595 events. Note a number of very high speed events (black). In order to compare with published results, we consider waves with phase speeds <500 m/s (red bars, 528).

- Wavelengths range from 200-600 km with a median of ~473 km.
- Phase speeds range from 60-250 m/s, with a median of ~137 m/s.
- Periods ranged from ~4 to > 100 min, with a median of ~60 min.

- The majority of the high phase speed (>500 m/s) waves (black lines) are propagating towards the east.
- The lower phase speed (< 500 m/s) MSTIDS (red lines) are seen to be propagating towards the east and southeast.

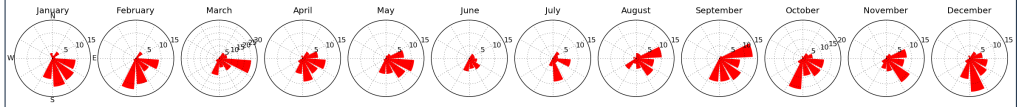

In order to investigate the monthly wave propagation distributions for the MSTIDs, we combined waves from 2010 – 2013 (total 33 months) into a single year and plotted them by month in 30° wide bins. For comparison, all data, except March and October, are plotted on the same scale.

- In each month the wave motions are predominantly southeastward.
- Variability in the wave propagation ranged from northeastward to southwestward.
- More waves were observed during the winter months with least occurrence in June and July.
- Remarkably no waves propagating in the northwest sector.

Discussion

Ishida et al. [2008] made observations of TIDs using two SuperDARN radars located in Alaska from December 2003 – February 2007. They observed 134 events almost all propagating southwards, but no northeast propagation.

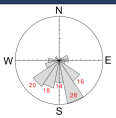

Ishida et al. [2008]

Frissell et al. [2014] made observations of mid-latitude TIDs using a SuperDARN radar located in Virginia (37° N) from June 2010 – May 2011. A majority of the TIDs observed were propagating towards the southeast at ~150°.

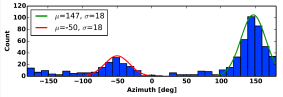

Frissell et al. [2014]

The propagation distribution of the TIDs obtained using PFISR show a majority of the waves to be propagating towards the southeast, similar to previous studies.

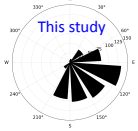

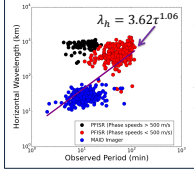

Wavelength vs. period from PFISR (black and red) and recent results from a co-located all-sky airglow imager (observations from 2011 – 2013) (blue) are shown along with a "global fit" (purple line) of optical, radar, and lidar measurements [e.g. *Reid*, 1986; *Taylor et al.* 1997]

Summary/Future Work

- Atmospheric gravity wave parameters were extracted from measured electron densities obtained from a number of different PFISR experiments run from August 2010 – April 2013.
- Over 500 MSTIDs were detected over the altitude range 100-300 km exhibiting well defined wave characteristics and dominant propagation directions towards the southeast.
- These propagation directions were found to be similar to other results obtained from SuperDARN radars in Alaska and Virginia.
- Wavelengths vs. periods from PFISR and a co-located all-sky airglow imager also agree will previous results.

Future work:

- Investigate wave characteristic as a function of altitude in 50 km altitude ranges from 100 – 300 km.
- Use spectral analysis to investigate other wave contributions.

References

- Frissell, N.A., J.B.H. Baker, J.M. Ruohoniemi, A.J. Gerrard, E.S. Miller, J.P. Marini, M.
- L. West, and W.A. Bristow (2014), Climatology of medium-scale traveling ionospheric disturbances observed by the midlatitude Balckstone SuperDARN radar, *J. Geophys. Res., 119*, 7679-7697, doi:10.1002/2014JA019870.
- Fritts, D.C. and M. J. Alexander (2003), Gravity wave dynamics and effects in the middle atmosphere, *Rev. Geophys. 41*, 1003, doi:10.1029/2001RG00106.
- Ishida, T., K. Hosokawa, T. Shibata, S. Suzuki, N. Nishitani, and T. Ogawa (2008), SuperDARN observations of daytime MSTIDs in the auroral and mid-latitudes: Possibly of long-distance propagation, *Geophys. Res. Lett., 35*, L13102, doi:10.1029/2008GL034623.
- Nicolls, M. J. and C. J. Heinselman (2007), Three-dimensional measurements of traveling ionospheric disturbances with the Poker Flat Incoherent Scatter Radar, *Geophys. Res. Lett., 34*, L21104, doi:10.1029/2007GL031506.
- Ried, I. M. (1986), Gravity wave motions in the upper middle atmosphere (60-110 km), *J. Atmos. Terr. Phys. 48* (11-12), 1057.
- Taylor, M. J., W. R. Pendleton, S. Clark, H. Takahashi, D. Gobbi, R. A. Goldberg (1997), Image measurements of short-period gravity waves at equatorial latitudes, *J. Geophys. Res. 102*, D22.
- Vadas, S. and D. C. Fritts (2005), Thermospheric responses to gravity waves: Influences of increasing viscosity and thermal diffusivity, *J. Geophys. Res., 110*, D15103, doi:10.1029/2004JD005574.

Acknowledgments

This project was funded by the National Science Foundation (NSF), Office of Polar Programs Grant OPP-1023265 titled "Collaborative Research: an Investigation of Wave Dynamics in the Arctic Mesosphere and Coupling Between the Lower and Upper Polar Atmosphere" (PI: K. Nielsen, UVU) Michael R. Negale is also supported by the NSF Graduate Research Fellowship under Grant #1147384.


Simulator
McEntire
Methods
Me and Dad got 2 pieces of wood. We carved it into 4 pieces. Then we glued it together. Then we got glass. We carved it a little, then we painted it. Then we got dry ice. We put the dry ice into the hot water. We turned the fan on, and it made a tornado.
Findings
This experiment taught me lots of things that you have to have in order for a tornado to form. The tornado simulator doesn't work if you don't have:
• All four sides of the box.
• The cracks between the glass.
• The fan on.
Conclusion
Tornados are powerful storms that need just the right conditions for them to form.
Cookies
Parakeet Diet
Simple
Machines

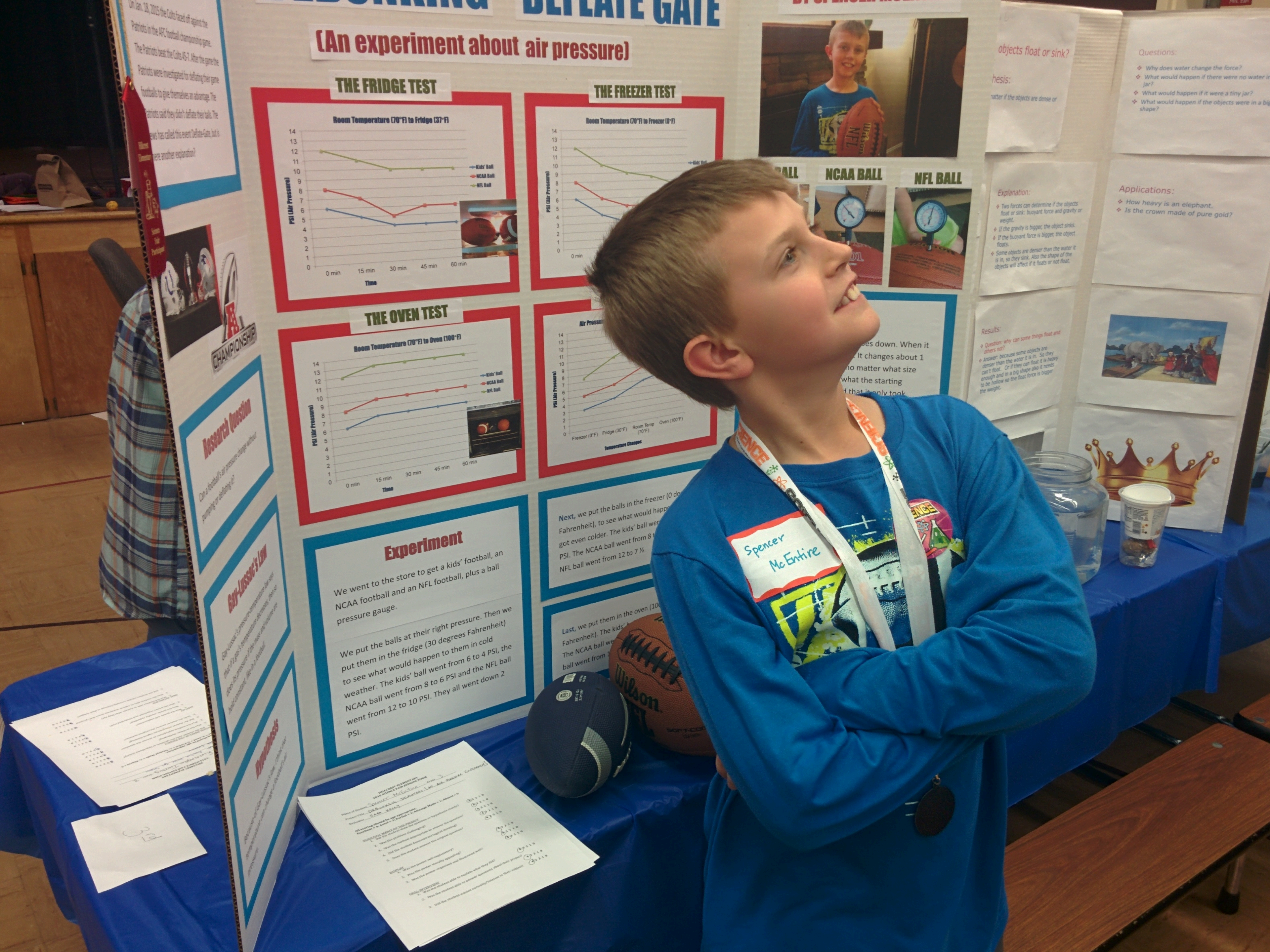

(An experiment about air pressure)
THE FRIDGE TEST
Room Temperature (70°F) to Fridge (37°F)
PSI (Air Pressure)
0 min
15 min
30 min
45 min
60 min
Time
Kids' Ball
NCAA Ball
NFL Ball
THE FREEZER TEST
Room Temperature (70°F) to Freezer (0°F)
THE OVEN TEST
Room Temperature (70°F) to Oven (100°F)
Freezer (0°F)
Fridge (30°F)
Room Temp (70°F)
Oven (100°F)
Temperature Changes
NCAA BALL
NFL BALL
Research Question
Gay-Lussac's Law
Hypothesis
Experiment
We went to the store to get a kids' football, an NCAA football and an NFL football, plus a ball pressure gauge.
We put the balls at their right pressure. Then we put them in the fridge (30 degrees Fahrenheit) to see what would happen to them in cold weather. The kids' ball went from 6 to 4 PSI, the NCAA ball went from 8 to 6 PSI and the NFL ball went from 12 to 10 PSI. They all went down 2 PSI.
Next, we put the balls in the freezer (0 de
Fahrenheit), to see what would happ
got even colder. The kids' ball wen
PSI. The NCAA ball went from 8
NFL ball went from 12 to 7 ½.
Last, we put them in the oven (10
Fahrenheit). The kids'
objects float or sink?
Questions:
Why does water change the force?
What would happen if there were no water in jar?
What would happen if it were a tiny jar?
Applications:
How heavy is an elephant.
Is the crown made of pure gold?
Explanation:
Results:
Spencer McEntire


0
2
4
6
8
10
12
14
16
18
20
0.2
0.4
0.6
1.0
1.2
1.4
bar
WILSON.COM
NATIONAL FOOTBALL LEAGUE
AMERICAN FOOTBALL CONFERENCE
NATIONAL FOOTBALL CONFERENCE
MADE IN CHINA


9:06

LEVEL 2:
BE INTERESTING.

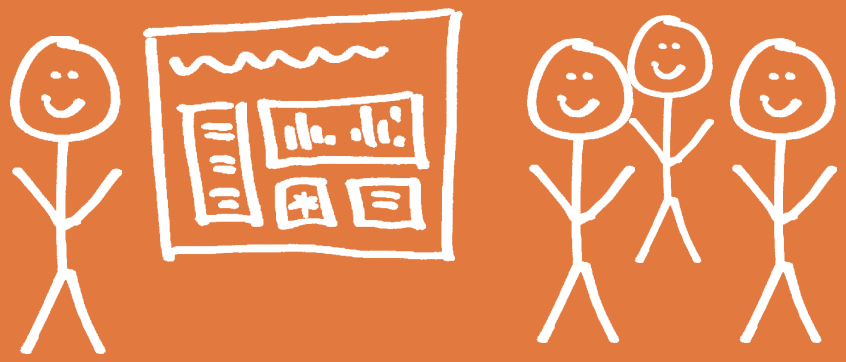

1. WOW WITH A TITLE.
2. BIG IMAGES, SIMPLE GRAPHS.
3. PULL QUOTES, KICKERS, ETC.

SELF-ADVOCACY SKILLS

LSL Teacher Perceptions: Preschool through Third-Grade

Ariel Hendrix, B.S. (M.Ed. Candidate) & Lauri Nelson, Ph.D.

> "Children with hearing loss should learn that they have a right and responsibility to access the same educational and social experiences as their peers."

INTRODUCTION

Self-advocacy is an essential component of social-emotional skill development. For children who are deaf or hard of hearing (DHH), self-advocacy is considered especially critical, as the broader population is not always understanding of their needs. Regardless of the severity of loss, all children who are DHH need to demonstrate the ability to self-advocate across settings and may require additional support in developing these skills. Age-appropriate self-advocacy skills can and should be introduced within early intervention home-based programs and within the preschool classroom to establish the foundation for future growth and development.

METHODS

A self-advocacy ratings questionnaire for young children who are DHH was developed and distributed to preschool through third-grade listening & spoken language teachers.

Participants included 12 teachers who offered their perceptions on the self-advocacy skills of their students with hearing loss (n = 64).

Teachers completed both quantitative and qualitative survey components that revealed information on:

- student skill level in hearing technology management, social and academic self-advocacy skills and proactive listening.
- frequency and type of self-advocacy goals listed in student Individualized Education Programs (IEPs)
- self-advocacy skills taught within the classroom
- impact of self-advocacy skill level on academic and social/emotional development
- teacher recommendations for fostering self-advocacy skill development.

RESULTS

Teacher perceptions of skill level increased from preschool to kindergarten across all three self-advocacy priority areas (see inset).

Skill level was generally higher in areas of self-advocacy that required a lower level of skill. Skills that required higher levels of responsibility, greater expressive communication or interaction with others were identified as general areas of weakness.

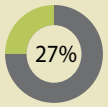

of students were reported to have self-advocacy goals written in their IEPs.

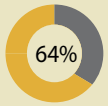

of students experienced negative effects on their academic and social/emotional development as a direct result of their self-advocacy skills.

For teachers who incorporated self-advocacy skills into their classroom instruction, a majority indicated that they focused on skills that required a lower level of responsibility or technical skill (e.g., consistent wearing of hearing technology, taking technology on/off), while very few identified more difficult skills as part of their curriculum (e.g., FM system responsibility, visual inspection of technology).

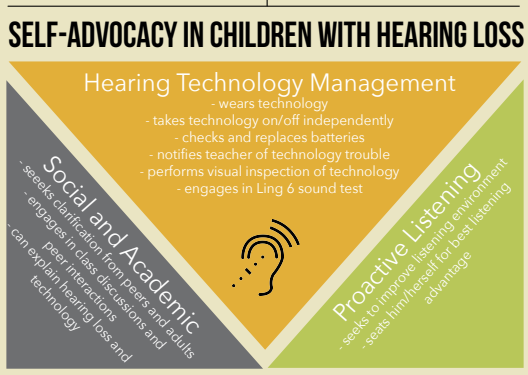

SKILL LEVELS

The following graphs indicate the frequency that each skill was mostly or always exhibited across age-groups:

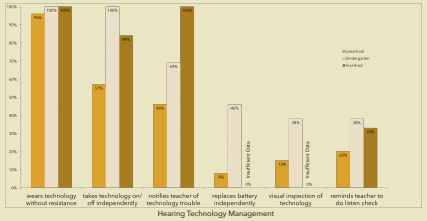

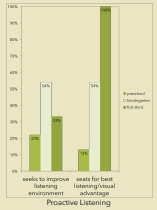

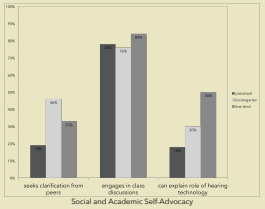

RECOMMENDATIONS

Children benefit when teachers foster age-appropriate self-advocacy skill development in their students across all self-advocacy priority areas and remain mindful that the level of self-advocacy skills attained in early childhood serve as a foundation for later success.

Children benefit when teachers utilize proper tools to identify areas of weakness in their students' level of self-advocacy skills and consciously incorporate them into IEP goal development and classroom instruction.

UtahState University

SELF-ADVOCACY SKILLS

LSL Teacher Perceptions: Preschool through Third-Grade

Ariel Hendrix, B.S. (M.Ed. Candidate) & Lauri Nelson, Ph.D.

> "Children with hearing loss should learn that they have a right and responsibility to access the same educational and social experiences as their peers."

INTRODUCTION

Self-advocacy is an essential component of social-emotional skill development. For children who are deaf or hard of hearing (DHH), self-advocacy is considered especially critical, as the broader population is not always understanding of their needs. Regardless of the severity of loss, all children who are DHH need to demonstrate the ability to self-advocate across settings and may require additional support in developing these skills. Age-appropriate self-advocacy skills can and should be introduced within early intervention home-based programs and within the preschool classroom to establish the foundation for future growth and development.

METHODS

A self-advocacy ratings questionnaire for young children who are DHH was developed and distributed to preschool through third-grade listening & spoken language teachers.

Participants included 12 teachers who offered their perceptions on the self-advocacy skills of their students with hearing loss (n = 64).

Teachers completed both quantitative and qualitative survey components that revealed information on:

- student skill level in hearing technology management, social and academic self-advocacy skills and proactive listening.
- frequency and type of self-advocacy goals listed in student Individualized Education Programs (IEPs)
- self-advocacy skills taught within the classroom
- impact of self-advocacy skill level on academic and social/emotional development
- teacher recommendations for fostering self-advocacy skill development.

RESULTS

Teacher perceptions of skill level increased from preschool to kindergarten across all three self-advocacy priority areas (see inset).

Skill level was generally higher in areas of self-advocacy that required a lower level of skill. Skills that required higher levels of responsibility, greater expressive communication or interaction with others were identified as general areas of weakness.

of students were reported to have self-advocacy goals written in their IEPs.

of students experienced negative effects on their academic and social/emotional development as a direct result of their self-advocacy skills.

For teachers who incorporated self-advocacy skills into their classroom instruction, a majority indicated that they focused on skills that required a lower level of responsibility or technical skill (e.g., consistent wearing of hearing technology, taking technology on/off), while very few identified more difficult skills as part of their curriculum (e.g., FM system responsibility, visual inspection of technology).

SKILL LEVELS

The following graphs indicate the frequency that each skill was mostly or always exhibited across age-groups:

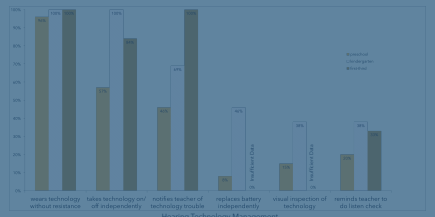

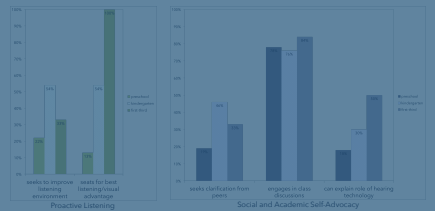

RECOMMENDATIONS

Children benefit when teachers foster age-appropriate self-advocacy skill development in their students across all self-advocacy priority areas and remain mindful that the level of self-advocacy skills attained in early childhood serve as a foundation for later success.

Children benefit when teachers utilize proper tools to identify areas of weakness in their students' level of self-advocacy skills and consciously incorporate them into IEP goal development and classroom instruction.

UtahState University

LEVEL 2:
BE INTERESTING.

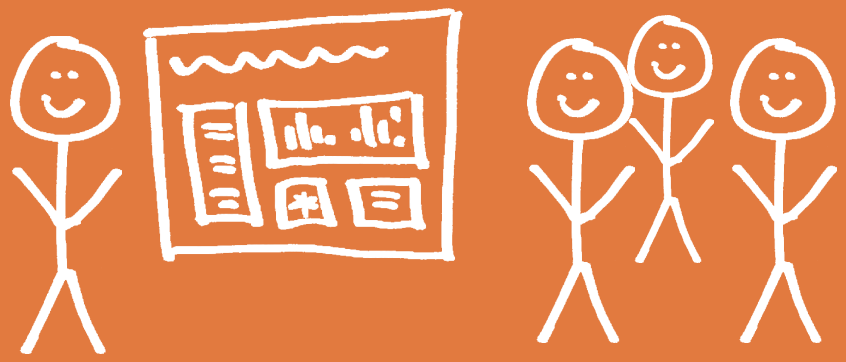

1. WOW WITH A TITLE.
2. BIG IMAGES, SIMPLE GRAPHS.
3. PULL QUOTES, KICKERS, ETC.